NASA CR-145161

COMPUTER PROGRAM TO SIMULATE RAMAN SCATTERING

By

Barbara Zilles and Roscoe Carter

March 1977

Prepared under Contract NAS1-13820

By

Old Dominion University Research Foundation
Norfolk, Virginia

for

NASA
National Aeronautics and
Space Administration

1. Report No.	2. Government Accession No.	3. Recipient's Catalog No.
NASA CR-145161		
4. Title and Subtitle COMPUTER PROGRAM TO SIMULATE RAMAN SCATTERING		5. Report Date January 1977
		6. Performing Organization Code
7. Author(s) Barbara Zilles and Roscoe Carter		8. Performing Organization Report No.
9. Performing Organization Name and Address Old Dominion University Research Foundation Norfolk, Virginia 23508		10. Work Unit No. 11. Contract or Grant No. NAS1-13820
12. Sponsoring Agency Name and Address National Aeronautics and Space Administration Washington, DC 20546		13. Type of Report and Period Covered Final Feb 26, 1975 to Oct 31, 1976 14. Sponsoring Agency Code
15. Supplementary Notes		

16. Abstract

A computer program is being developed to simulate the vibration-rotation and pure rotational spectrum of a combustion system consisting of various diatomic molecules and CO_2 as a function of temperature and number density. The main program for this purpose has been developed along with the necessary subroutines to generate two kinds of spectra--a pure rotational spectrum for any mixture of diatomic and linear triatomic molecules, and a vibrational spectrum for diatomic molecules. The program is designed to accept independent rotational and vibrational temperatures for each molecule, as well as number densities.

17. Key Words (Selected by Author(s))	18. Distribution Statement		
	Unclassified - Unlimited		
19. Security Classif. (of this report) Unclassified	20. Security Classif. (of this page) Unclassified	21. No. of Pages 59	22. Price*

*For sale by the National Technical Information Service, Springfield, VA 22161

TABLE OF CONTENTS

COMPUTER PROGRAM TO SIMULATE RAMAN SCATTERING

By

Barbara Zilles[1] and Roscoe Carter[2]

SUMMARY

A computer program is being developed to simulate the vibration-rotation and pure rotational spectrum of a combustion system consisting of various diatomic molecules and CO_2 as a function of temperature and number density. The main program for this purpose has been developed along with the necessary subroutines to generate two kinds of spectra--a pure rotational spectrum for any mixture of diatomic and linear triatomic molecules, and a vibrational spectrum for diatomic molecules. The program is designed to accept independent rotational and vibrational temperatures for each molecule, as well as number densities.

In the following section, the theory upon which the program is based is described in detail. In the third section block diagrams of the program are given. The different variables and functions are identified and their relation to the theory and/or logical flow of the computing format is explained. In the "results" section examples of computed spectra are given along with a brief description of the input parameters used to produce these spectra.

[1] Research Staff, Old Dominion University Research Foundation, Norfolk, Virginia 23508.

[2] Assistant Professor of Chemical Sciences, Old Dominion University, Norfolk, Virginia 23508.

THEORY

The power signal collected for a Raman transition from rotation-vibration state Jv to $J'v'$ is given by

$$R_{Jv}^{J'v'} = n\,\gamma_{Jv}\,V\bar{I}\Omega\varepsilon\left(\frac{d\sigma}{d\Omega}\right)_{Jv}^{J'v'} \tag{1}$$

where n = number density

γ_{Jv} = probability of finding a molecule in rotation-vibration state Jv according to the Maxwell-Boltzmann distribution law

V = irradiated volume

$\bar{I}$ = average intensity of irradiation in that volume

ε = efficiency of collecting optics

Ω = scattering angle in steradians

$\left(\frac{d\sigma}{d\Omega}\right)_{Jv}^{J'v'}$ = differential Raman cross section for the transition.

Optical Factor

The problem of defining a volume in the sample which interacts with the laser light and the average intensity within that volume has been considered by Barrett and Adams (ref. 1). They have shown that for a laser beam focused to a diffraction limited point by a lens of focal length equal to that of the collecting optics a cylindrical volume may be defined

$$V = 2bA_f \ , \tag{2}$$

where A_f is the area of the laser focal point and b is the distance in both directions along the beam axis at which the irradiance has dropped to $1/e^2$ its intial value. A_f is related to b by

$$b = 2A_f/\lambda \quad , \tag{3}$$

where λ is the wavelength of the laser line. The average intensity in this volume is found to be

$$\bar{I} = \frac{A_u}{A_f} \frac{\left[\tan^{-1}(2)\right] I_o}{8} \tag{4}$$

where A_u is the area and I_o the irradiance of the unfocused laser beam. Substituting equation (3) into equation (2) and combining with equation (4) gives

$$V\bar{I} = \frac{A_u A_f}{2\lambda} \left[\tan^{-1}(2)\right] I_o \quad .$$

Now, A_f is related to A_u by

$$A_f = 4\lambda^2 f^2 / A_u$$

where f is the focal length of the focusing lens. Hence we have

$$V\bar{I} = 2\lambda f^2 \left[\tan^{-1}(2)\right] I_o \quad . \tag{5}$$

The irradiance I_o is given by

$$I_o = P/A_u \tag{6}$$

where P is the laser power.

Frequency

The frequency associated with the transition giving rise to the signal in equation (1) may be separated into rotational and vibrational terms.

$$\omega_{Jv}^{J'v'} = \omega_{v}^{v'} + \omega_{J}^{J'}$$

$$= \left[G(v') - G(v)\right] + \left[F_{v'}(J') - F_{v}(J)\right] \tag{7}$$

where G and F_v are the vibrational and rotational energies, respectively, of the states in question. The rotational energy depends on the vibrational as well as the rotational quantum numbers:

$$F_v(J) = B_v J\ (J + 1) \tag{8}$$

If B_o is the rotational constant of the ground vibrational state,

$$B_v = B_o - \sum_i \alpha_i\ v_i \tag{9}$$

where α_i is the vibration-rotation interaction constant and v_i is the vibrational quantum number for the ith normal mode of vibration.

For the pure rotational spectrum, of course, $v' = v$ and $\omega_v^{v'} = 0$. For vibrational spectra the transitions will involve a change of quantum number for only one normal mode (that is, combination bands will not be considered). Thus, dropping the normal mode subscript for $\Delta v = v' - v$ and α, the rotational part of the transition frequencies for the different branches of the band are as given in table 1. [B_v in the table, however, still denotes a sum over normal modes as in equation (9)].

The vibrational energy relative to that of the ground state is given by

$$G^{o}(v) = \sum_i \left[\omega_i^o - x_{ii}^o - \frac{1}{2} \sum_{j \neq 1} x_{ij}^o\right] v_i - \sum_i \sum_{j \leq i} x_{ij}^o\ v_i\ v_j \tag{10}$$

Table 1.

Branch	J'	$\omega_J^{J'}$ (a)	$S_{JJ'}^{\ell}$ (b)
O	J-2	$-4B_v(J - \frac{1}{2}) - \alpha(J - 1)(J - 2)\Delta v$	$\frac{3}{2}\frac{(J^2 - \ell^2)[(J - 1)^2 - \ell^2]}{J(J - 1)(2J - 1)(2J + 1)}$
P	J-1	$-2B_vJ - \alpha J(J - 1)\Delta v$	$\frac{3\ell^2(J^2 - \ell^2)}{J(J + 1)(J - 1)(2J - 1)}$
Q	J	$-\alpha J(J + 1)\Delta v$	$\frac{[J(J + 1) - 3\ell^2)]^2}{J(J + 1)(2J - 1)(2J + 3)}$
R	J+1	$2B_v(J + 1) - \alpha(J + 1)(J + 2)\Delta v$	$\frac{3\ell^2[(J + 1)^2 - \ell^2]}{J(J + 1)(J + 2)(2J + 1)}$
S	J+2	$4B_v(J + \frac{3}{2}) - \alpha(J + 2)(J + 3)\Delta v$	$\frac{3}{2}\frac{[(J + 1)^2 - \ell^2][(J + 2)^2 - \ell^2]}{(J + 1)(J + 2)(2J + 1)(2J + 3)}$

(a) From equations (7), (8), and (9).

(b) From Placzek, reference 3.

where ω_i^o is the harmonic frequency of the ith vibrational mode and x_{ij}^o the anharmonicity constant for the interaction of modes i and j. For the band involving transitions of the kth normal mode, therefore, the vibrational part of the transition frequency is given by

$$\omega_v^{v'}(k) = \omega_k^o \Delta v - x_{kk}^o (2v_k + \Delta v + 1)\Delta v - \sum_{i \neq k} x_{ik}^o (v_i + \tfrac{1}{2})\Delta v$$

where Δv denotes the quantum number change, that is, $\Delta v = v_k' - v_k$. For the fundamental band of a diatomic molecule, there is only one normal mode and $\Delta v = 1$. Hence the above equation becomes

$$\omega_v^{v'} = \omega^o - 2x^o (v + 1) \quad . \tag{11}$$

Boltzmann Factor

The population of the Jv rotation-vibration state is given by

$$\gamma_{Jv} = \left[g_J (2J + 1)\, e^{-F(J)/kT_r}\, e^{-G^o(v)/kT_v} \right] / Z_r Z_v^o \tag{12}$$

where g_J is the nuclear degeneracy of the rotational state, T_r is the rotational temperature, and T_v is the vibrational temperature. $F_v(J)$ and $G^o(v)$ are the rotational energy and the vibrational energy relative to the zero point energy, respectively. Z_r is the rotational partition function and Z_v^o is the vibrational partition function relative to the zero point population. The rotational partition function can be approximated by an integral (see for example ref. 2, Appendix C):

$$\begin{aligned} Z_r &= \sum_J g_J (2J + 1) \prod_i e^{-(B_o - \alpha_i v_i) J (J+1)/kT_r} \\ &\approx \tfrac{1}{2} kT_r (g^+ + g^-) / \sum_i (B_o - \alpha_i v_i) \end{aligned} \tag{13}$$

where g^+ and g^- are the nuclear degeneracies of the even and odd J levels. Thus the partition function product is equal to

$$Z_r Z_v^o = \frac{1}{2} kT_r \, (g^+ + g^-) \, Z(T_v)$$

$$Z(T_v) = \sum_v \frac{g_v e^{-G^o(v)/kT_v}}{B_o - \sum_i \alpha_i v_i} \tag{14}$$

where $G^o(v)$ is given by equation (10) and g_v is the vibrational degeneracy--which equals 1 except for states (occurring in CO_2) where a degenerate normal mode, k, is excited, $g_v = v_k + 1$.

Cross Section

The differential scattering cross section in equation (1) is given by (ref. 3):

$$\left(\frac{d\sigma}{d\Omega}\right)_{Jv}^{J'v'} = 2^4 \pi^4 \omega_R^4 \; |\langle J'v'|\alpha|Jv\rangle|^2 \quad . \tag{15}$$

ω_R is the scattered Raman frequency,

$$\omega_R = \frac{1}{\lambda} + \omega_{Jv}^{J'v'} \tag{16}$$

where λ is the exciting wavelength and $\omega_{Jv}^{J'v'}$ is the frequency of the transition given by equation (7).

$\langle J'v'|\alpha|Jv\rangle$ is the matrix element of the polarizability tensor for the initial and final vibration-rotation states in the laboratory-fixed system. In terms of the molecule-fixed coordinate system the diagonal tensor element (scattered light polarized parallel to the incident electric vector) is given by

$$\alpha_{ZZ} = \sum_{ij} \cos(i,Z) \; \alpha_{ij} \cos(j,Z) \tag{17}$$

For linear and symmetric top molecules, if α_{ij} is broken down into a sum of spherical and traceless tensors (ref. 3)

$$|\langle J'v'|\alpha_{ZZ}|Jv\rangle|^2 = |\langle v'|\alpha|v\rangle|^2 \delta_{JJ'} + \frac{4}{45} |\langle v'|\beta|v\rangle|^2 S_{JJ'} \tag{18}$$

where $\delta_{JJ'}$ is the Kronecker delta and $S_{JJ'}$ is the rotational line strength. The parameters, α and β, referred to as the polarizability and anisotropy, respectively, are two invariants of the polarizability tensor $\hat{\alpha}$

$$\alpha = \frac{1}{3} \text{tr } \hat{\alpha} = \frac{1}{3} \sum_j \alpha_{jj}$$

$$\beta = \frac{1}{2} \left[3\text{tr } (\hat{\alpha} \hat{\alpha}^\dagger) - (\text{tr } \hat{\alpha})^2 \right] \tag{19}$$

They are functions of the normal vibration coordinates Q and may be developed in a power series

$$\alpha(Q) = \alpha_o + \left(\frac{\partial \alpha}{\partial Q}\right)_o Q + \ldots$$

$$\beta(Q) = \beta_o + \left(\frac{\partial \beta}{\partial Q}\right)_o Q + \ldots ,$$

Thus

$$|\langle v'|\alpha|v\rangle|^2 = \alpha^2 \delta_{vv'} + \alpha'^2 |\langle v+1|Q|v\rangle|^2 \delta_{v',v+1} \tag{20}$$

where the zero subscript has been dropped. For a diatomic molecule the normal coordinate matrix element is given by

$$|\langle v+1|Q|v\rangle|^2 = \frac{Nh(v+1)}{8\pi^2 c\omega^o \mu} \tag{21}$$

where N = Avogadro's number

h = Planck's constant

c = speed of light

ω^o = the harmonic frequency as in equations (10) and (11)

μ = the reduced mass.

Similarly, the anisotropy for any molecule may be expanded

$$|\langle v'|\beta|v\rangle|^2 = \beta^2 \delta_{vv'} + \beta'^2 |\langle v+1|Q|v\rangle|^2 \delta_{v',v+1} \tag{22}$$

The first term in equation (22) when substituted into the second term in equation (18) gives the pure rotational spectrum for parallel polarization. The first term in equation (20) gives the contribution to the Rayleigh scattering.

The second terms in equations (20) and (22) determine the vibrational spectrum. For perpendicular polarization the off-diagonal polarizability tensor element α_{YZ} in the laboratory system is considered using a transformation analogous to equation (17). For linear and symmetric top molecules,

$$|\langle J'v'|\alpha_{YZ}|Jv\rangle|^2 = \frac{3}{45} |\langle v'|\beta|v\rangle|^2 S_{JJ'} \quad . \tag{23}$$

Thus for vibrational spectra we can define trace and anisotropic scattering cross sections:

$$\left(\frac{d\sigma}{d\Omega}\right)_{trace} = \left(\frac{d\sigma}{d\Omega}\right)_{||} - \frac{4}{3}\left(\frac{d\sigma}{d\Omega}\right)_{\perp} = |\langle v'|\alpha|v\rangle|^2 \delta_{JJ'} \tag{24}$$

$$\left(\frac{d\sigma}{d\Omega}\right)_{anis} = \frac{45}{3}\left(\frac{d\sigma}{d\Omega}\right)_{\perp} = |\langle v'|\beta|v\rangle|^2 S_{JJ'} \tag{25}$$

where the parallel and perpendicular cross sections are determined by whether the component of α in equation (15) is ZZ or YZ, respectively.

For the diatomic molecules in this study, the parallel scattering contains significant contributions from the anisotropic as well as the trace cross sections. For polyatomic molecules $\alpha_i' = \frac{\partial \alpha}{\partial Q_i}\Big)_o$ depends on the normal coordinate being considered. It is always greatest for the totally symmetric vibration. For spherical top molecules, $\beta_i = 0$ for the strong totally symmetric vibration and thus only the trace scattering need be calculated.

For asymmetric top molecules the anisotropic scattering does not assume such a simple form as equation (25). However, for H_2O, the asymmetric top considered in this study, the anisotropic scattering is weak compared to the trace scattering and does not contribute to the appearance of the spectrum [the depolarization ratio = $I_\perp/I_\parallel$ is 0.02 (ref. 4)]. The experimental trace scattering may be determined quantitatively since the relation in equation (24) still applies. Hence for H_2O, only the trace scattering will be calculated.

The rotational line strength factors $S_{JJ'}$ are determined by the matrix elements of the direction cosines as seen from equations (17) and (18). They determine the rotational selection rules. For pure rotational spectra the selection rules are

$$\Delta J = J' - J = \pm 2 \tag{26}$$

for the diatomic molecules. Since the antistokes scattering ($\Delta J = -2$) is symmetrical to the stokes scattering ($\Delta J = +2$), except for the ω_R^4 factor in equation (15) and the Boltzmann factor, it gives no new information and is not calculated.

For the triatomic linear CO_2 molecule, those states where the doubly degenerate bending mode, ν_3, is excited, can have non-zero vibrational angular momentum quantized along the figure axis. This angular momentum vector contributes to the direction cosine matrix

elements in the same way as the quantized component of the rotational angular momentum for a symmetric top. Thus for states with a non-zero vibrational angular momentum quantum number ℓ the line strengths depend on ℓ as well as J and J' and we have the selection rules

$$\Delta J = \pm 1 \quad \text{for} \quad \ell \neq 0 \tag{27}$$

in addition to equation (26).

For CO_2 states with $v_3 \neq 0$, there are $v_3 + 1$ states with the same energy. When v_3 is odd all the states have $\ell \neq 0$ and there are two states each with $|\ell| = 1, 3, 5, \ldots v_3$. When v_3 is even there is one state with $\ell = 0$ and two states each with $|\ell| = 2, 4, 6, \ldots v_3$. For the pairs of states with the same ℓ value, a given J level of only one of the states is occupied for CO_2, since one state is symmetric with respect to interchange of the identical oxygen nuclei and one state is antisymmetric. Since oxygen has zero nuclear spin, only the even J levels are occupied for symmetric states and only the odd J levels for antisymmetric states. States with $\ell = 0$ are symmetric.

In addition to different nuclear degeneracies, states with different ℓ have different line strength factors so that $S_{JJ'}$ in equation (18) is given by

$$S_{JJ'} = \sum g_J^{\ell} S_{JJ'}^{\ell} \quad . \tag{28}$$

The $S_{JJ'}^{\ell}$ are given in table 1 for $\Delta J = 0, \pm 1, \pm 2$; they reduce to the line strength factors for diatomic molecules when $\ell = 0$. For rotational spectra $J' = J + 1, J + 2$; for vibrational spectra all five branches are calculated.

Units and Summary

In equation (1) $R_{Jv}^{J'v'}$ is in watts, since $V\overline{I}$ is in watt-cm, n is in cm^{-3} and the cross section is in cm^2. We may obtain intensity in photons/sec by dividing by

1 photon at frequency $\omega_R = hc\omega_R$ watt-sec

where h is in joule-sec, c is in cm/sec, and ω_R is given by equation (16).

In summary then, for rotational spectra the signal in counts/sec is

$$R_{Jv}^{J'v'} = \frac{Cn}{Z}\,\omega_R^3\, g_J(2J+1)e^{-F(J)kT_r}\, e^{-G^o(v)/kT_v}\,(S_{JJ'}) \qquad (29)$$

where $Z = Z_r Z_v^o/k$ and

$$C = 2^4\pi^4\,\frac{4}{45}\,\beta^2\,\frac{V\bar{I}\Omega\varepsilon}{khc} \quad . \qquad (30)$$

For vibrational spectra of diatomic molecules the O and S branch signals are

$$R_{Jv}^{J'v'} = \frac{C'n}{Z}\,\omega_R^3\,\frac{A(v+1)}{\omega^o\mu}\, g_J(2J+1)e^{-F(J)/kT_r}\, e^{-G^o(v)kT_v}\left(S_{JJ'}\right) \qquad (31)$$

where $A = Nh/8\pi^2c$ and C' is the same as C except that β is replaced by β'.

The signal for the vibrational Q branch is the same as equation (31) except that $S_{JJ'}$ is replaced by

$$11.25\,\alpha'^2/\beta'^2 + S_{JJ} \quad .$$

PROGRAMMING

The computer program consists of a main program to take care of the major input/output operations, calculate general constants and manage the general flow of operations; a subroutine, PART, to calculate the partition functions; a subroutine, LINES, to generate the corresponding frequency and intensity arrays; a subroutine, CNVLUT,

to convolute with the line shape function; a subroutine, SLIT, to convolute with the slit function; and a subroutine, SPKPLT, to plot the resulting spectrum.

The program is set up so that for a given run only a given type of spectra may be computed. The alternatives are:

1. a set of pure rotational spectra for any combination of diatomic or linear triatomic molecules,
2. a set of vibrational spectra for diatomic molecules,
3. a set of vibrational spectra for CO_2,
4. a set of vibrational spectra for H_2O,
5. a set of vibrational spectra for CH_4.

Thus a different LINES subroutine is placed in the card deck according to the desired option. At present the LINES subroutine has been completed only for the first two options.

Main Program

A flow chart of the main program is shown in figure 1. The input parameters and the constants calculated in the main program are as follows:

Instrument parameters. λ, exciting wavelength in Å; P, laser power in watts; A_ℓ, area of unfocused laser beam in cm^2; Ω, collecting angle in steradians; f, focal length of focusing lens in cm; ε, total efficiency.

Optical factor. $F = 2\lambda\left[\tan^{-1}(2)\right] \times 10^{-8}\ f^2\Omega P\varepsilon/A_\ell$. See equation (5).

Spectrum parameters. DX, plotting increment in cm^{-1}; $\Delta\omega$, halfwidth of the line shape function in cm^{-1}; RLIM, limit of intensity in counts/sec, below which R for a given line is set equal to zero; SLT, spectral halfwidth of the slit in cm^{-1}; ALNGTH, length of the plotted spectrum in inches; NSTRT, frequency in cm^{-1} at which spectrum begins; IEND, frequency in cm^{-1} at which spectrum ends.

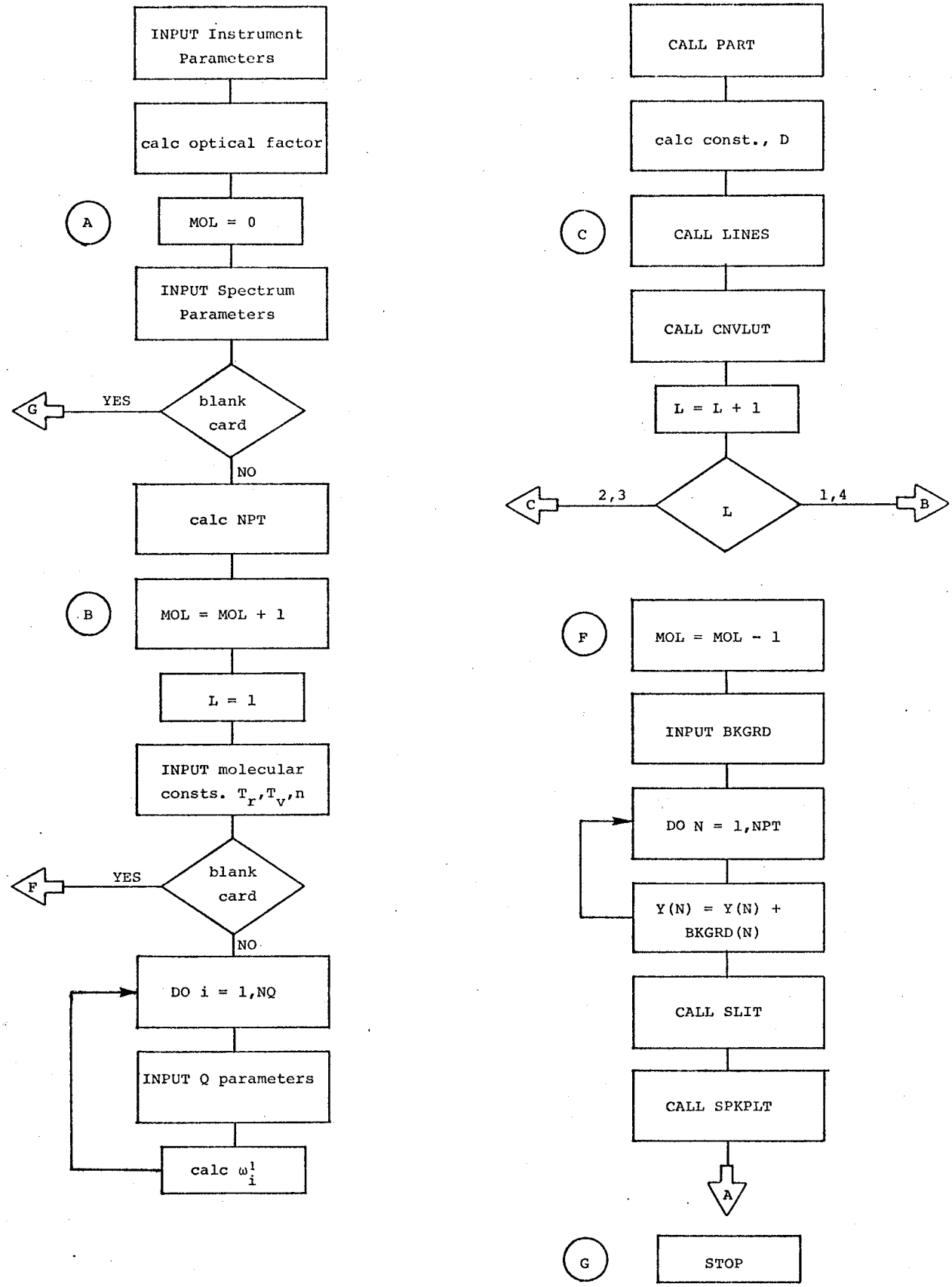

Figure 1. Flow chart for main program.

NPT is the number of plotting points. NPT = (NSTRT - IEND)/DX + 1.

Molecular constants. B_o, ground state rotational constant in cm^{-1}; β or β', anisotropy in cm^3 for pure rotational spectra or anisotropy derivative in cm^2 for vibrational spectra; ATB, $(\alpha'/\beta')^2$, zero for a pure rotational spectrum; μ, reduced mass--zero for a pure rotational spectrum; NQ, number of normal coordinates--must be 1 or 3; g^+ and g^-, nuclear degeneracy of positive and negative J levels, respectively; NJ, maximum J quantum number; SPECIE, name of molecule.

T_r = rotational temperature; T_v = vibrational temperature; n = number density in molecules/cm^3.

Normal mode, Q, parameters. $\omega^o(Q_i)$, harmonic vibration frequency in cm^{-1}; $x^o(Q_i)$, anharmonicity constant in cm^{-1}; $\alpha(Q_i)$, rotation-vibration interaction constant in cm^{-1}; $NS(Q_i) = +1$ or -1, symmetry of normal coordinate with respect to reflection through a plane containing the figure axis. If the symmetry of the vibrational wave function is negative, the nuclear degeneracies of the odd and even J levels are interchanged. This symmetry is given by

$$n_s = \prod_i NS(Q_i)^{v_i} \quad . \tag{32}$$

NVM(i), maximum v quantum number for the ith vibrational mode.

ω_i^1 is a factor used in the PART and LINES subroutines,

$$\omega_i^1 = \omega_i^o - x_{ii}^o \tag{33}$$

$$D = 2^4\pi^4 \frac{4\ \beta^2 nF}{45\ khc\ Z} \quad . \tag{34}$$

See equations (29) and (30).

The index L in the main program serves to manage the generation and convolution of the different branches of a vibrational spectrum. In the rotational LINES subroutine the R branch, if allowed, is

calculated simultaneously with the S branch; hence it sets L to zero so that at the L flag in the main program the flow will be recycled to begin generation of lines for another molecule if desired or to plot the spectrum.

Similarly, if only the trace scattering of the vibrational spectrum is to be generated for H_2O (because the anisotropic scattering is impracticable) or for CH_4 (because the anisotropy is zero), L will be set to zero in the LINES subroutine and only the Q branch will be generated. For vibrational spectra in which the anisotropic as well as trace scattering is to be computed, L = 1, 2, 3 correspond to the O, Q, and S branches, respectively.

The index MOL is introduced primarily for the case of the pure rotational spectrum where the scattering from several molecules appears in the same spectral region. It serves to index the specie concentrations and temperatures for labeling of the plotted spectrum.

The addition of the background, BKGRD, to the array of spectral ordinates, Y, has not yet been implemented as this data is not available. It is presently assumed that the data will be deconvoluted and hence the background is added between the line shape and slit function convolutions.

PART Subroutine

The subroutine PART calculates Z, the rotational times the vibrational partition function divided by the Boltzmann constant k. A flow chart of this subroutine is given in figure 2. The variables calculated are as follows:

num = numerator of $Z(T_v)$ without g_v [see equation (14)]

$$\text{num} = \prod_i e^{-(\omega_i^1 - x_{ii}^o v_i)v_i/kT_v} \tag{35}$$

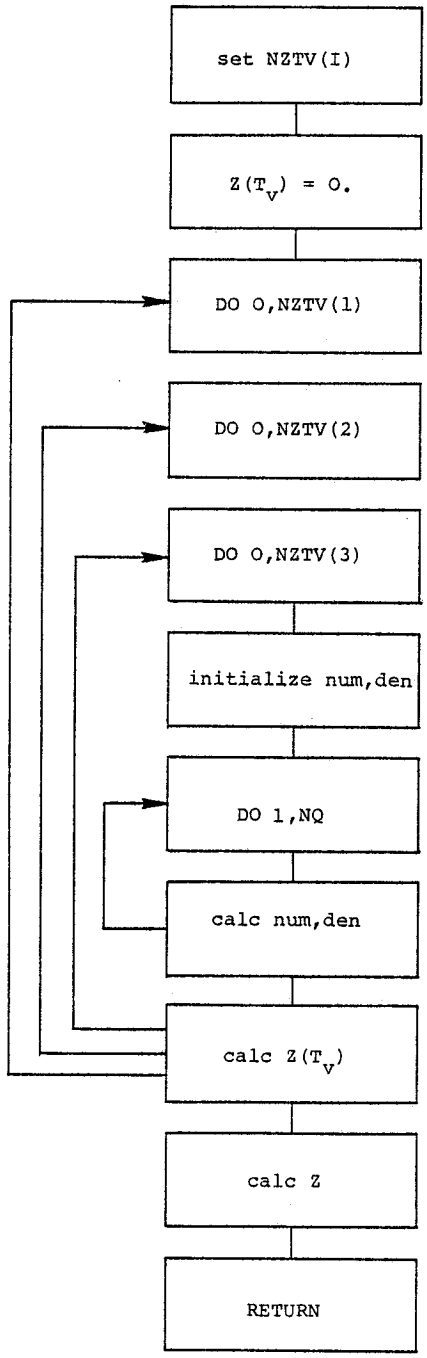

Figure 2. Flow chart for subroutine PART.

as in equation (10) where it is assumed that $x^{o}_{ij} = 0$ for $i \neq j$, and ω^{1}_{j} is given by equation (33).

den = denominator of $Z(T_v)$ $\qquad$ $den = B_o - \sum_i \alpha_i v_i$

$$Z(T_v) = \sum_v \frac{num(v)(v_3 + 1)}{den(v)}$$

$$Z = \frac{Z_r Z^o_v}{k} = T_r \frac{(g^+ + g^-)}{2} Z(T_v)$$

The sums and products in this function are performed numerically. Theoretically the sum over vibrational levels is infinite. In practice NVM(I), the maximum v quantum number, is input so that the population of this level is less than 10^{-6} that of the ground state. NZTV(I) is then set equal to NVM(I) +3 and higher contributions to the sum should be negligible. If there is only one normal coordinate (diatomic case) NZTV(2) = NZTV(3) = 0.

Rotational LINES Subroutine

The rotational LINES subroutine calculates the frequencies and intensities of the spectral lines for the R (CO_2) and S branches according to equation (29) and table 1. A flow chart of this subroutine appears in figure 3. Its rather complicated appearance is due to the accomodation of linear triatomic molecules with their three degrees of vibrational freedom and non-zero vibrational angular momentum. The loops over quantum numbers for the different vibrational modes are nested in order of decreasing frequency $\omega_1 > \omega_2 > \omega_3$. The loop over J is nested within the loops over v, and the loops for summing over the degenerate vibrational substates (ℓ quantum number) as in equation (28) are nested within the J loop. The parameters and functions calculated are as follows.

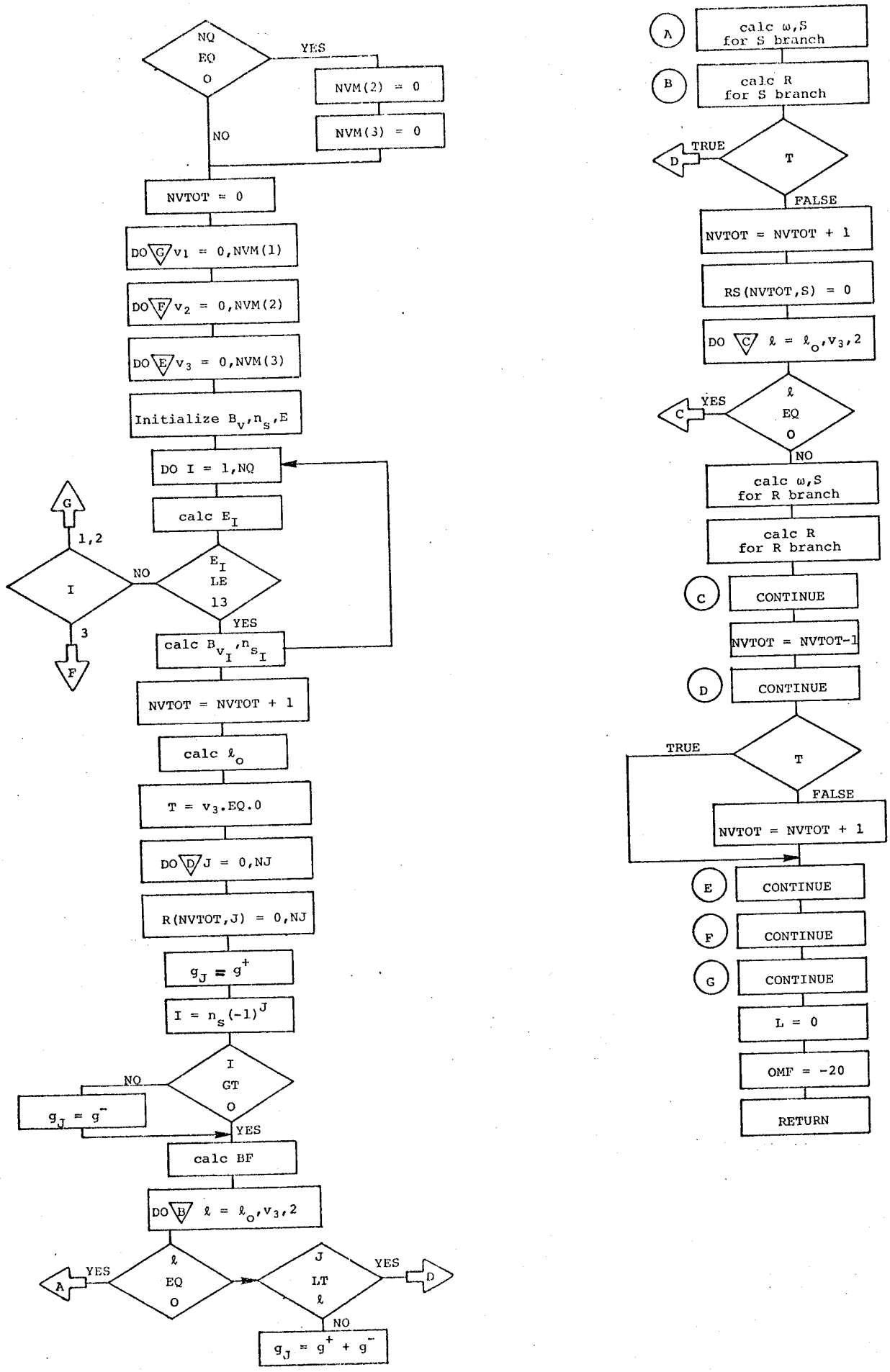

Figure 3. Flow chart for rotational LINES subroutine.

NVTOT is the index of vibrational states for all the different v_1, v_2, v_3 and also for the R and S branches. Thus if $\omega_{Jv}^{J+2,v}$ is given by $\omega(\text{NVTOT},J)$, $\omega_{Jv}^{J+1,v}$ is given by $\omega(\text{NVTOT}+1,J)$. Thus NVTOT must be decremented for each cycle over J if $v_3 \neq 0$ and must be re-incremented before initiating a new cycle over v_3.

B_v is given by equation (9) and n_s is given by equation (32).

E is the exponent in the vibrational part of the Boltzmann factor [see equation (35)],

$$E_i = \sum_{j \leq i} (\omega_j^1 - x_{jj}^o \, v_j) v_j \quad .$$

If the above sum exceeds 13 for a given v_3, then any states with the same v_1, v_2 values will have even higher populations for higher v_3, so control is transferred out of the v_3 loop; similarly for v_2. For v_1 control is transferred to the end of its loop.

$\ell_o = 1$ for v_3 odd; $\ell_o = 0$ for v_3 even as in the discussion following equation (27).

T is a logical variable, tested for calculating R branches and processing NVTOT.

g_J is the nuclear degeneracy set equal to g^+ or g^- according to whether the vibration-rotation product wavefunction is symmetric or antisymmetric. After the contribution to R for the $\ell = 0$ state for a given v_3 has been calculated, g_J is set equal to $g^+ + g^-$ since $\ell \neq o$ states occur in pairs as discussed following equation (27).

BF is the Boltzmann factor without g_J and the (2J+1) factor which cancels with that in the denominator of S_{JJ}^{ℓ}, for the R and S branches (see table 1).

(J.LT.ℓ) is a logical variable which if true transfers control to the end of the J loop, since J is the total angular momentum quantum number and states with $J < \ell$ cannot exist.

$\omega_J^{J'}$ and S_{JJ}^{ℓ}, are as given in table 1 with $\Delta v = 0$, except that the (2J+1) factor in the denominator of S_{JJ}^{ℓ}, has been cancelled out.

R is given by equation (29) using the factors which have been calculated:

$$R(NVTOT,J) = \sum_{\ell} D \left(\frac{1}{\lambda} - \omega(NVTOT,J) \right)^3 g_J^{\ell}(BF) S_{JJ}^{\ell},$$

where D was calculated in the main program according to equation (34).

Vibrational LINES Subroutine

The vibrational LINES subroutine calculates the frequency and intensity of the spectral lines for the O, Q, and S branches of a diatomic molecule according to equation (31). The flow chart is given in figure 4. It follows the same general form as the rotational routine without the sums and products over multiple vibrational coordinates and allowing for the difference in formulas. The variables calculated are as follows.

DD is the constant factor D in equation (34) weighted by the normal coordinate matrix element, as given by equation (21), without the (v+1) factor.

ω_F is the vibrational part of the transition frequency for $v = 0$, $\omega_F = \omega^1 - x^o$ according to equations (11) and (33).

IEX is a factor used in calculating c_2 (see below), IEX = -1 for L = 1; IEX = 1 for L = 3.

c_1 is the coefficient for the J independent terms in the frequency formulas for the O and S branches, $c_1 = B_v - \alpha$.

ω_v is the vibrational part of the transition frequency, $\omega_v = \omega_F - 2x^o v$.

ω_c includes the J independent terms from the rotational part of the transition frequency, $\omega_c = \omega_v + 2c_1 L$.

c_2 is the coefficient of the frequency terms linear in J, $c_2 = 4c_1(IEX) - \alpha$.

H is the DD factor weighted by (v+1)--see above.

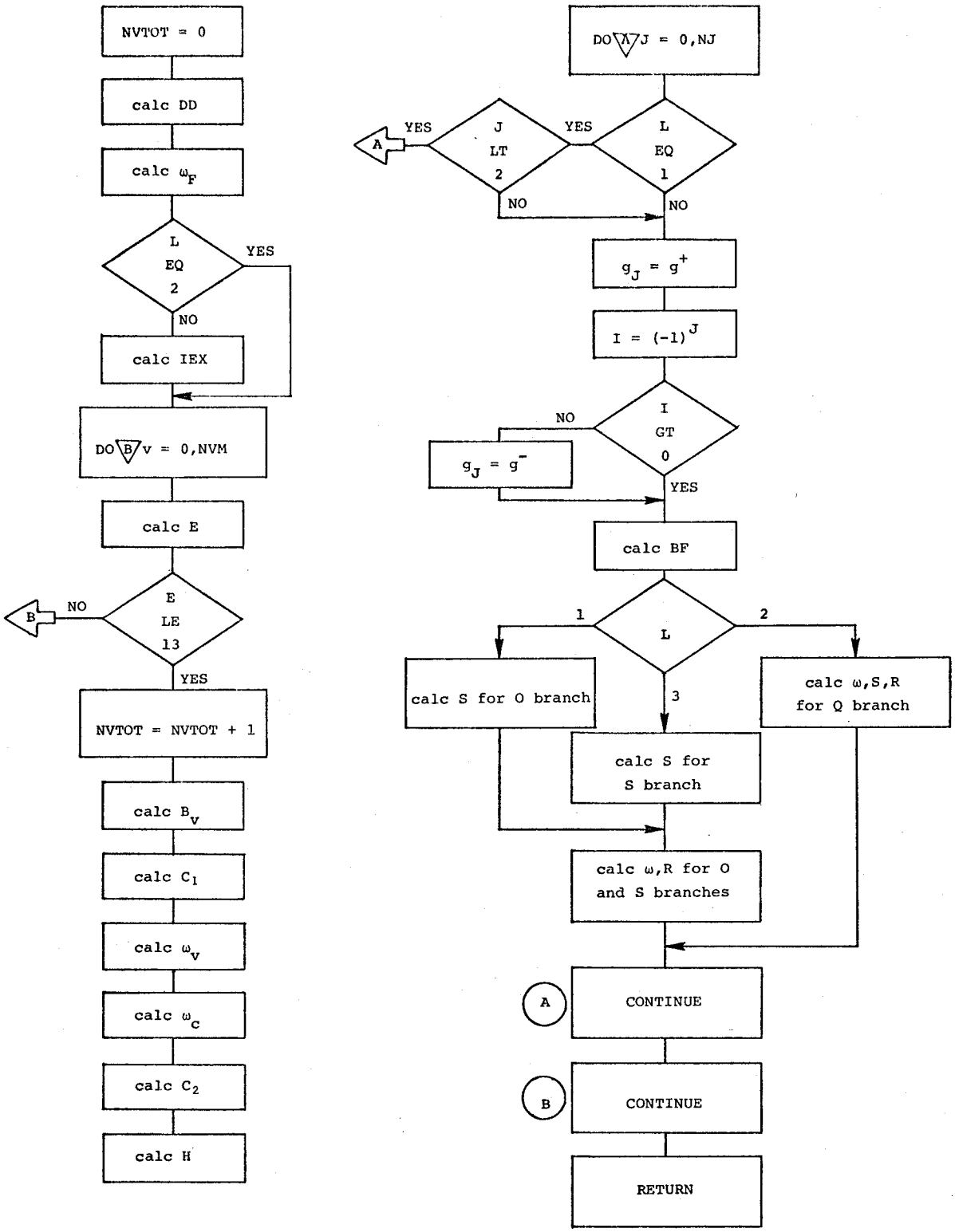

Figure 4. Flow chart for vibrational LINES subroutine.

(J.LT.2) is a logical variable tested to eliminate negative J" values for the O branch (J' = J + 2).

g_J and BF are the same as in the rotational subroutine.

$\omega_J^{J'}$ and $S_{JJ'}$ are as given in table 1, with $\ell = 0$ and $\Delta v = 1$, $\omega = \omega_c + c_2 J - \alpha J^2$ for the O and S branches. And $\omega = \omega_v - \alpha J(J+1)$ for the Q branch. The (2J+1) factor in denominator of $S_{JJ'}$ for the O and S branches has been cancelled out with that in BF as in the rotational subroutine.

R is given by equation (31) using the factors which have been calculated. Thus for the O and S branches,

$$R(NVTOT,J) = H\left(\frac{1}{\lambda} - \omega(NVTOT,J)\right)^3 g_J(BF)S_{JJ'} .$$

And for the Q branch,

$$R(NVTOT,J) = H(2J+1)\left(\frac{1}{\lambda} - \omega(NVTOT,J)\right)^3 g_J(BF)(11.25\ ATB + S_{JJ}).$$

where $ATB = (\alpha'/\beta')^2$.

CNVLUT Subroutine

The CNVLUT subroutine calculates the ordinates Y(N) of the spectrum by convoluting over the generated lines with a Lorentzian line shape function. The flow chart is given in figure 5.

(MOL.EQ.1) and (L.GE.2) are flags which insure that the cumulated data are saved from a previous molecule (pure rotational spectra) or from previously convoluted branches (vibrational spectra). Otherwise the array of ordinates, Y(N), is initialized to zero.

YMAX saves the maximum ordinate value for scaling the spectrum before plotting and labeling it.

X is the abscissa in cm^{-1}.

(J.LT.2) has the same function as in the vibrational LINES subroutine.

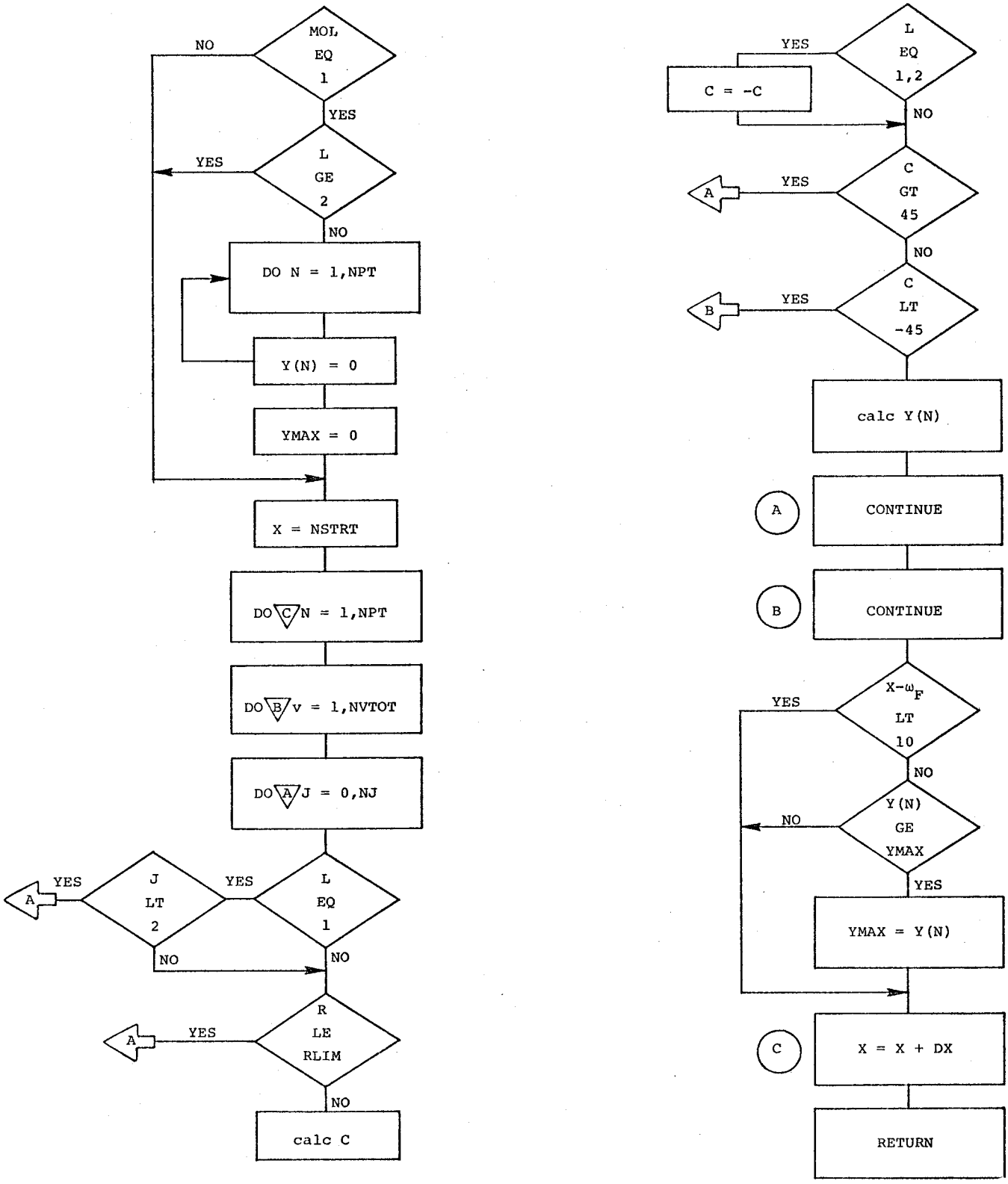

Figure 5. Flow chart for subroutine CNVLUT.

The Y(N) values for each point are calculated according to

$$Y(N) = \sum_{v} \sum_{J} \frac{R(v,J)\,(\Delta\omega)^2}{(\Delta\omega)^2 + [\omega(v,J) - X]^2}$$

The C and RLIM flags are to eliminate unnecessary calculations in this time-consuming routine, $C = X - \omega(v,J)$. If $|C| > 45$ the contribution of $R(v,J)$ to $Y(N)$ is neglected. If $\omega(v,J) < X$ $(C > 0)$, the program skips over J values until ω is brought within the range of 45 cm^{-1} from X, since ω increases with increasing J values. If $\omega(v,J) > X$ $(C < 0)$, then once $|C| > 45$ cm^{-1} no higher J values will bring it into this range so control is transferred outside the J loop to the next v -- $\omega(v,J)$ decreases with increasing v. Actually for the O and Q branches ω decreases with increasing J (see table 1). The (L.EQ.1) or (L.EQ.2) flag, therefore, sets $C = -C$ so that the C flags will have the same effect for the O and Q branches as for the R and S branches.

The $(X - \omega_F)$ flag allows for truncating the Q branch of a vibrational spectrum so that the structure of the rotational wings can be observed. Thus an ordinate is not considered maximum unless it is 10 or more cm^{-1} from the v = 0 line (ω_F) of the Q branch. In the rotational LINES subroutine ω_F is set equal to -20 so that $(X - \omega_F)$ will never be less than 10.

SLIT and SPKPLT Subroutines

The SLIT subroutine is set up analogous to CNVLUT except that the convolution function is triangular rather than Lorentzian and the sum is over the data points generated by CNVLUT rather than the quantum numbers. It also generates and stores an array of abscissa values, X(N), corresponding to Y(N). At present there seems to be something wrong with this subroutine as the program has never

completed a run since it was added. The DEC-10 computer throws the job off the system without leaving a LOG:FILE or any record of the job having been logged on.

The SPKPLT subroutine generates a PLOT:FILE from the ordinate and abscissa arrays. It consists primarily of subroutine calls which are specific to the DEC-10 system. This subroutine is currently being rewritten for use on the CDC-6000 computer and is not given here.

RESULTS

Examples of computed spectra appear in figures 6 through 14. For all these spectra the same instrument parameters were used. They are:

exciting line	= 4880 Å
laser power	= 0.5 watts
area of unfocused laser beam	= 0.0128 cm^2
collecting angle	= 0.05 steradians
focal length	= 50 cm
efficiency	= .10

The convolution over the triangular slit function was not performed for these spectra. Only a single convolution with the Lorentzian line shape was performed, but the halfwidth used was typical of (the lower limit of) spectral slitwidths, that is, 0.5 cm^{-1}--whereas natural line widths would be on the order of 0.01 to 0.1 cm^{-1}. A typical plotting increment was .2 cm^{-1}. RLIM was chosen as 1×10^{-6} for the vibrational spectra and 1×10^{-3} for the pure rotational spectra.

The molecular parameters used in the computed spectra are given in table 2 and the normal coordinate parameters in table 3. The B_o, α, ω_i^o, and x_{ii}^o values were derived from analysis of

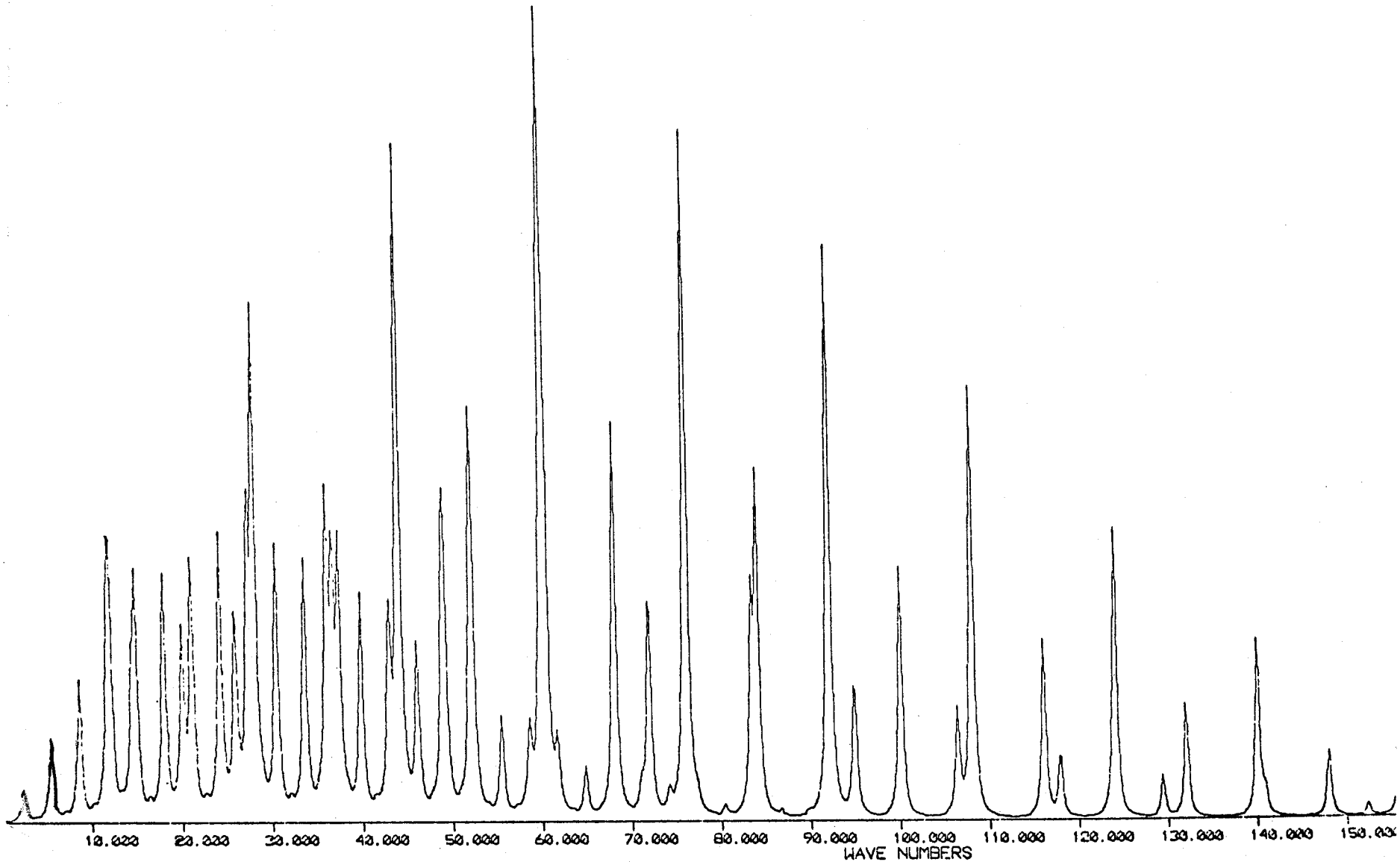

Figure 6. Rotational Raman spectrum of 78% N_2, 15% O_2, 7% CO_2 at 298 °K.

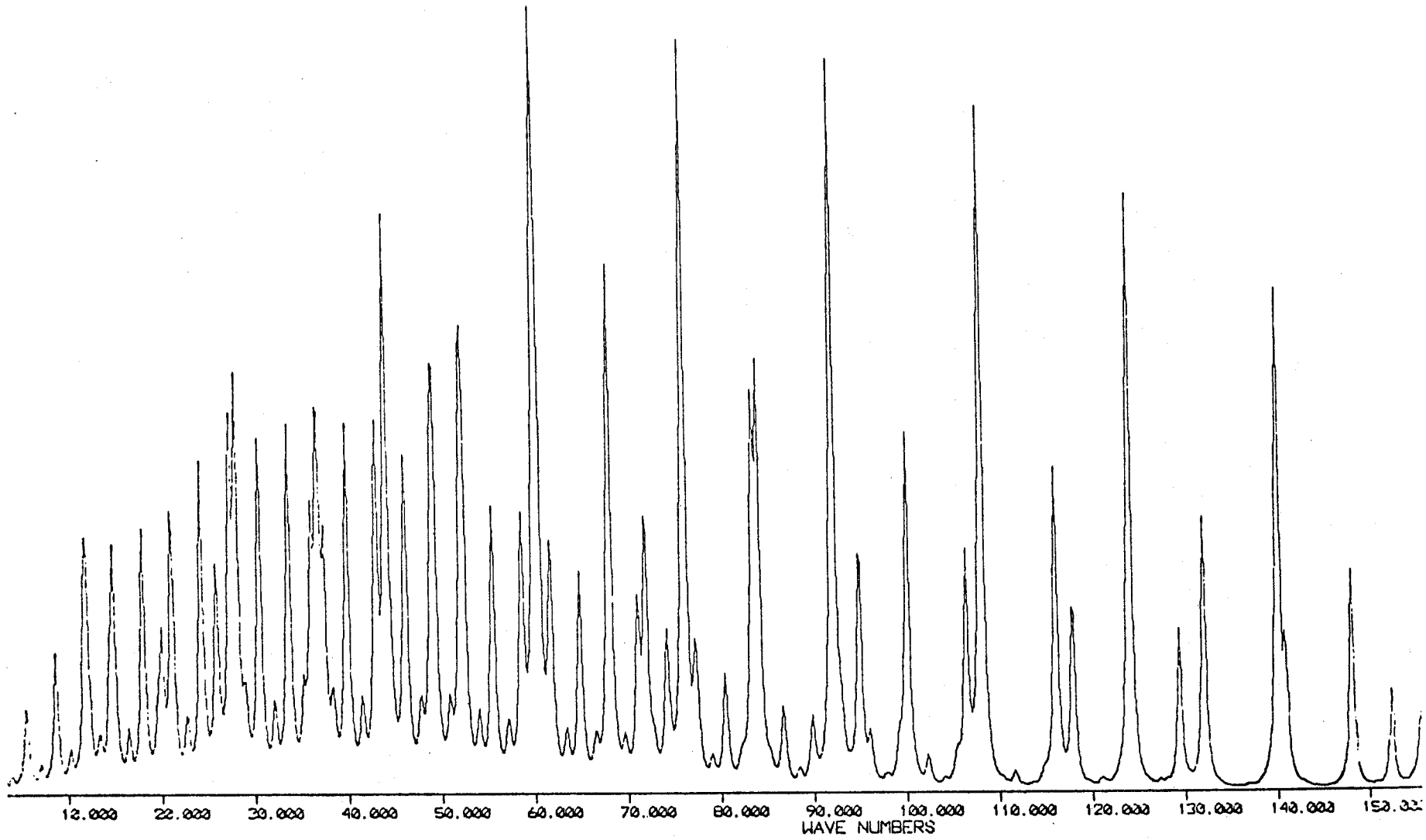

Figure 7. Rotational Raman spectrum of 78% N_2, 15% O_2, 7% CO_2 at 600 °K.

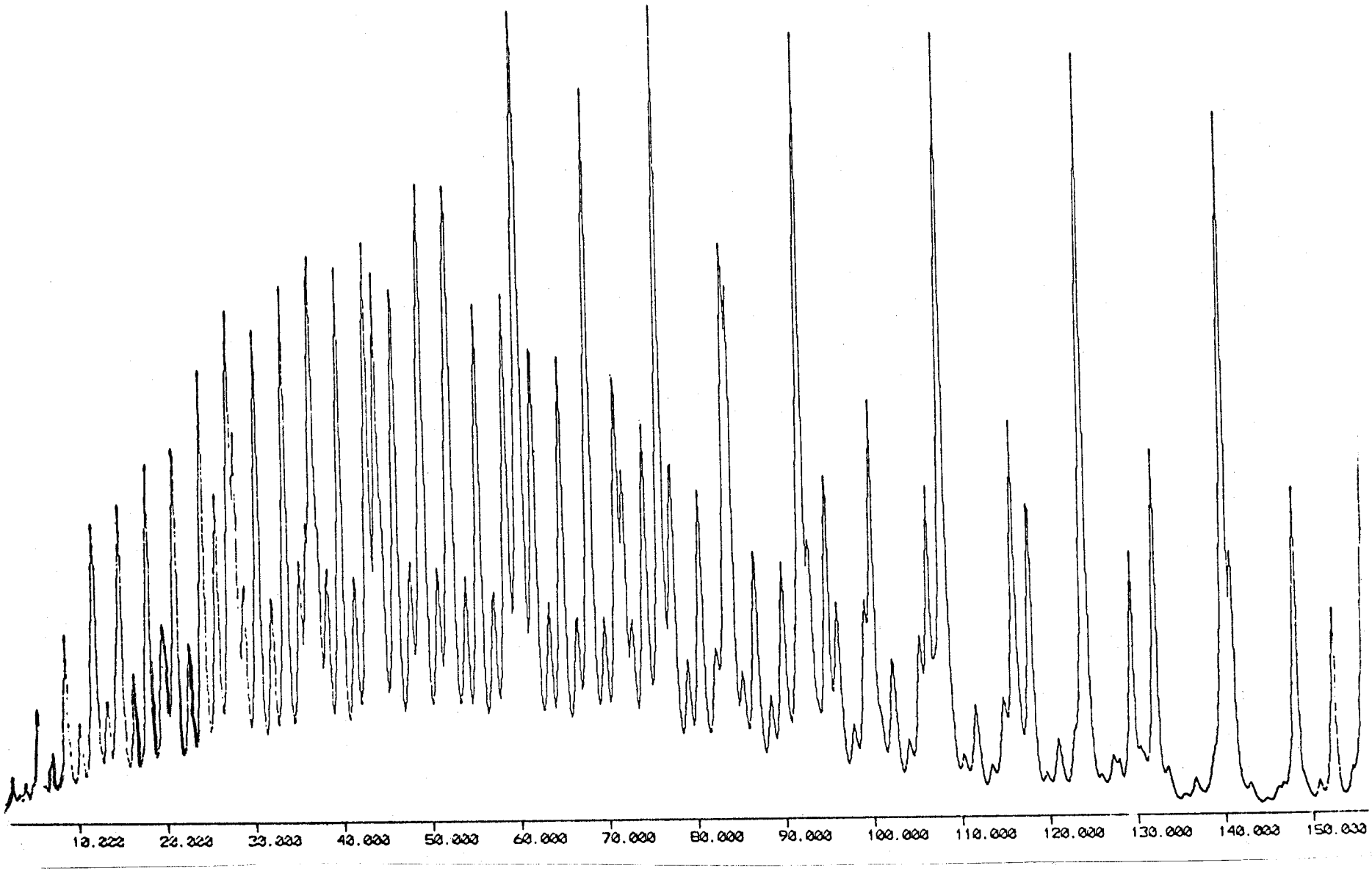

Figure 8. Rotational Raman spectrum of 78% N_2, 15% O_2, 7% CO_2 at 1000 °K.

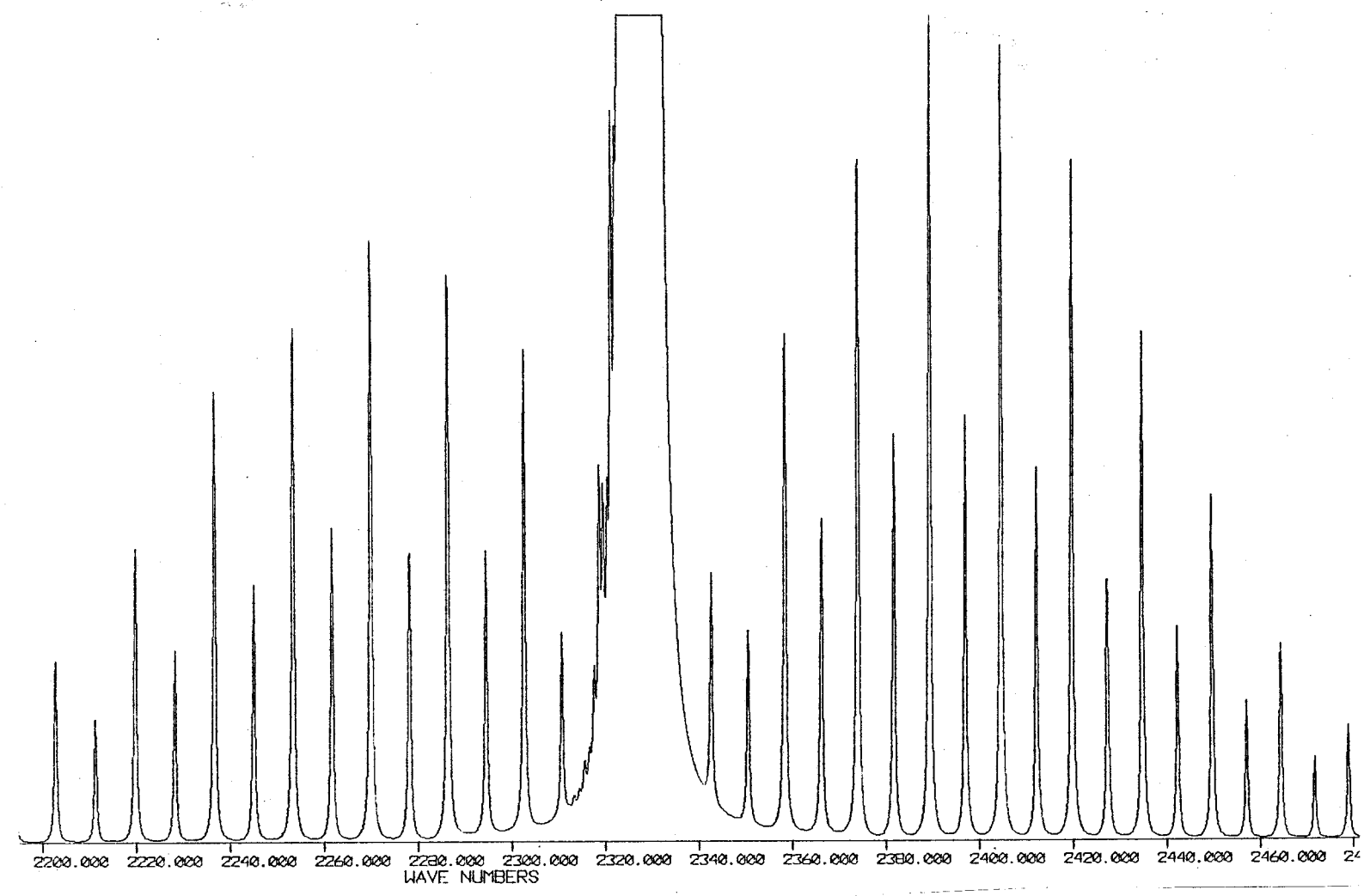

Figure 9. Vibrational Raman spectrum of N_2 at 298 °K.

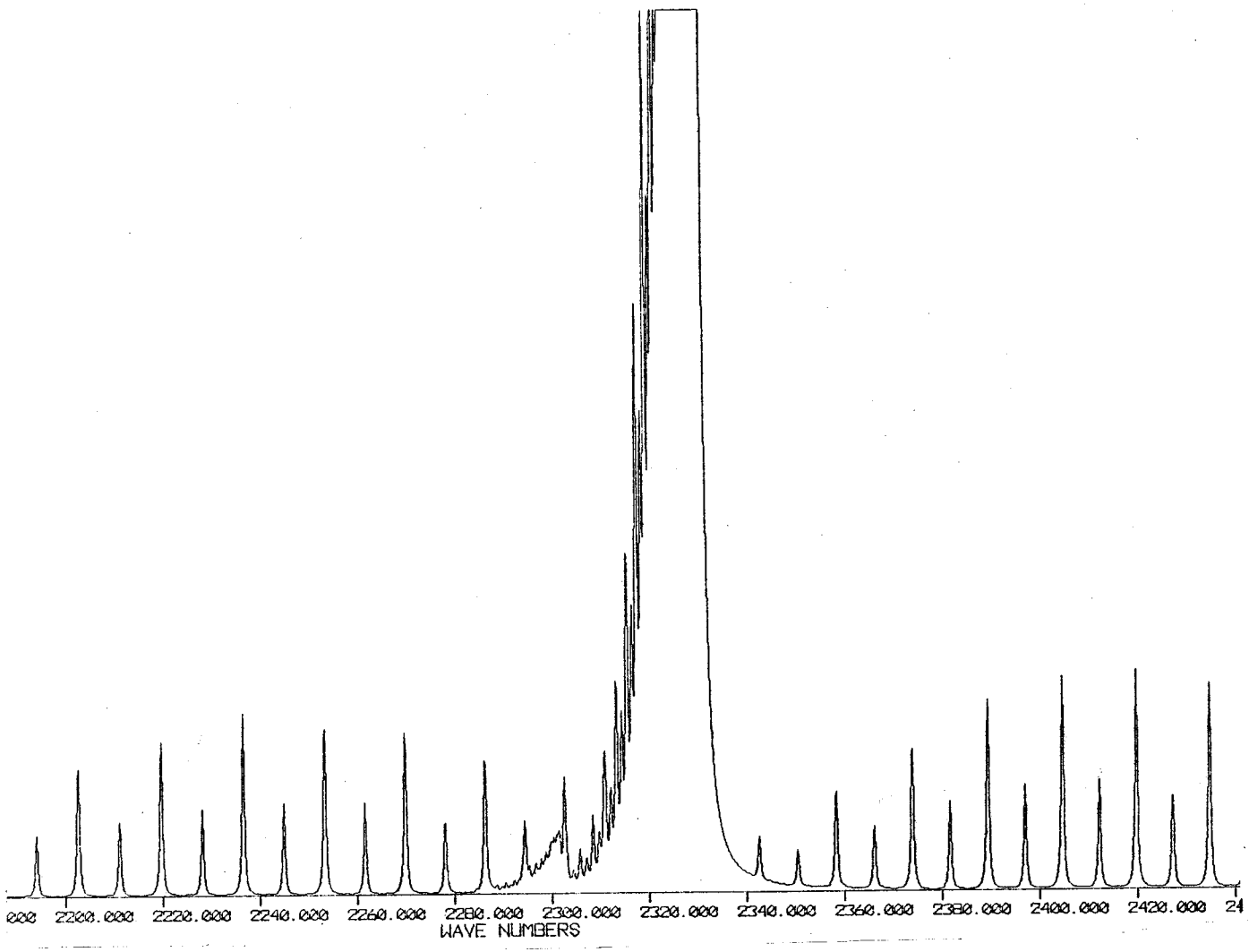

Figure 10. Vibrational Raman spectrum of N_2 at 600 °K.

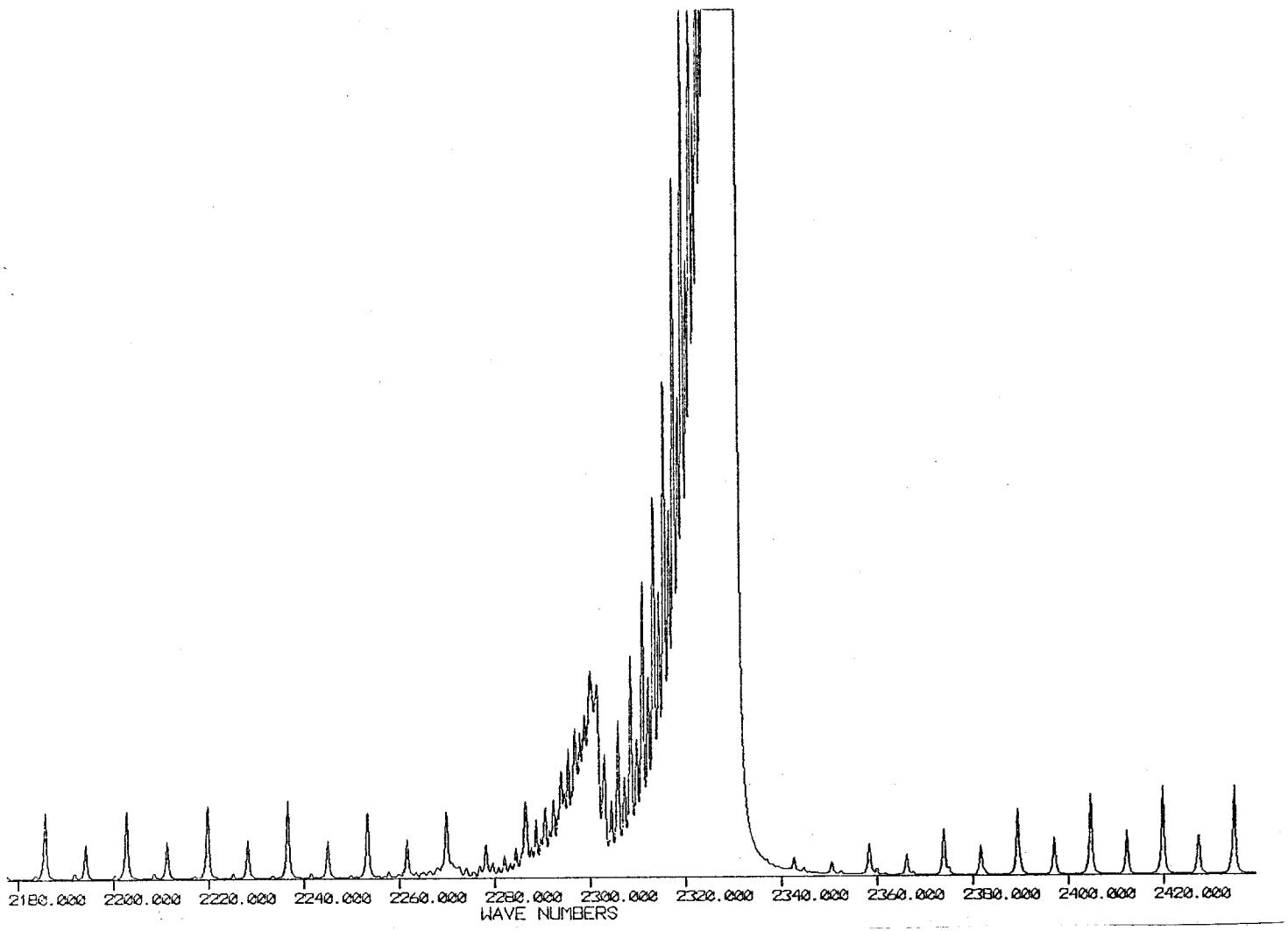

Figure 11. Vibrational spectrum of N_2 at 1000 °K.

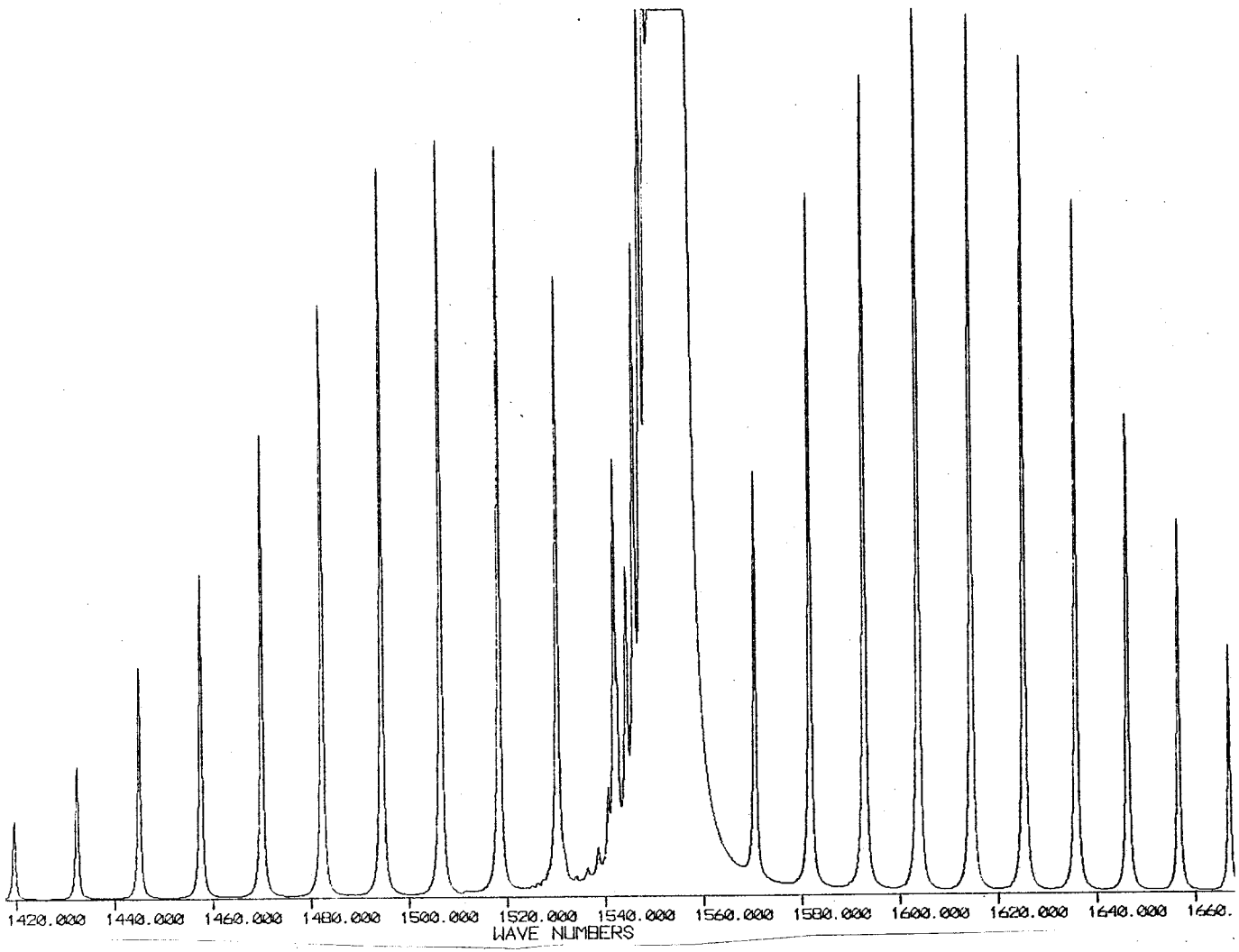

Figure 12. Vibrational Raman spectrum of O_2 at 298 °K.

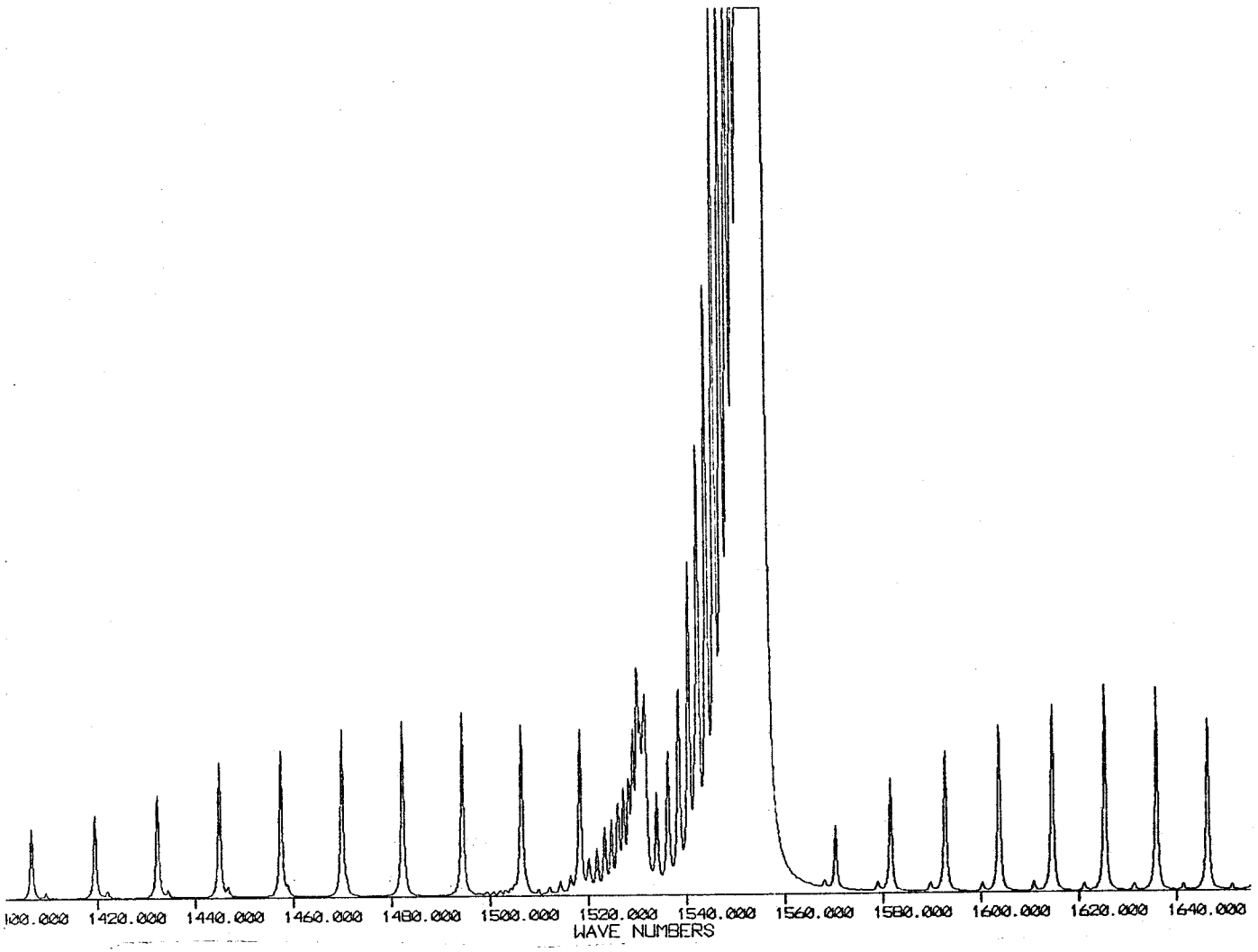

Figure 13. Vibrational Raman spectrum of 0 at 600 °K.

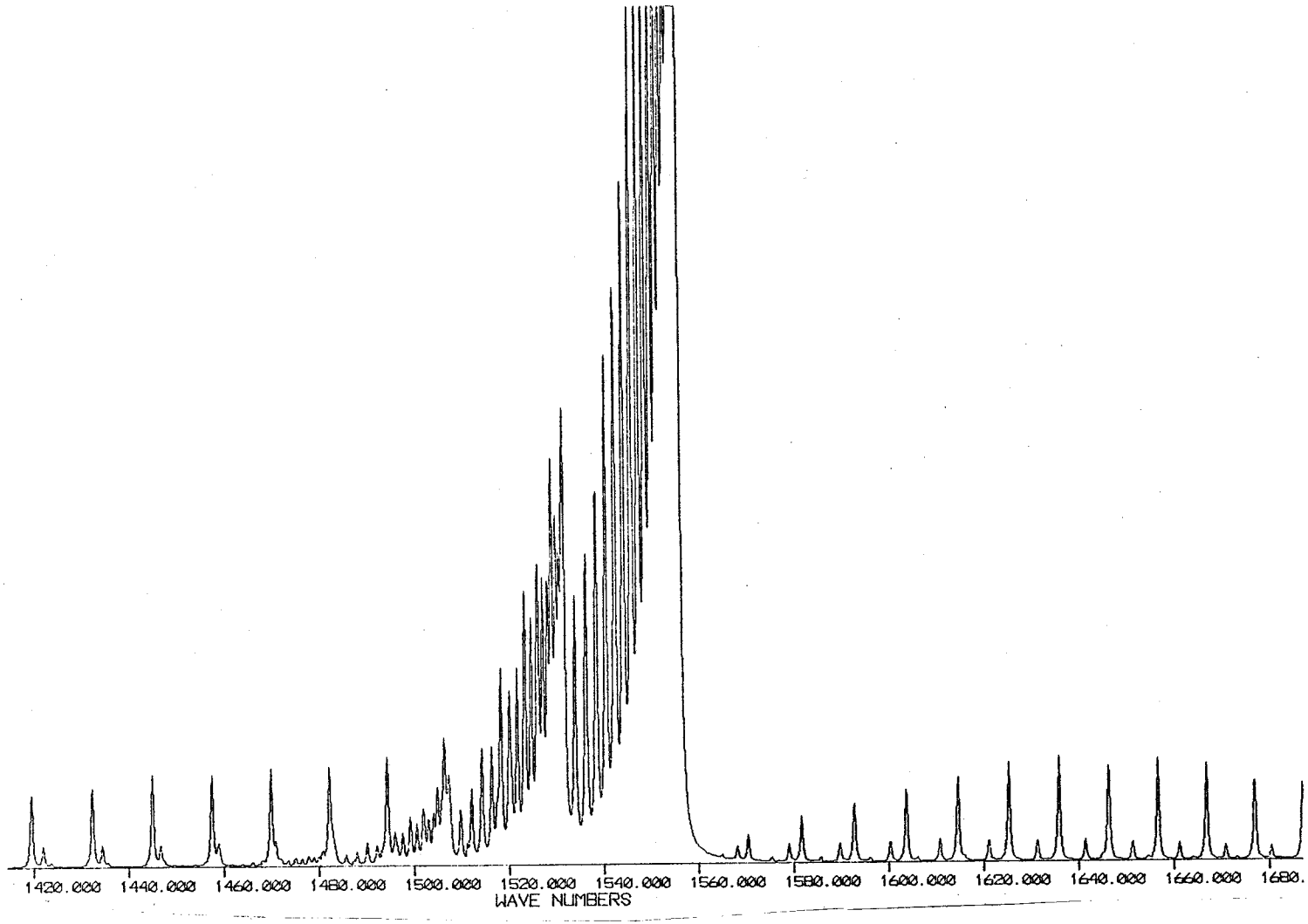

Figure 14. Vibrational Raman spectrum of O_2 at 1000 °K.

Table 2

	$B_o cm^{-1}$	$\beta, 10^{-24} cm^3$ [b]	$\beta', 10^{-16} cm^2$ [b]	ATB [b]	g^+	g^-
N_2	2.00065 [a]	.950	2.16	.546	6	3
O_2	1.43776 [a]	1.18	2.34	.357	0	1
CO_2	.39021 [c]	2.44			1	0

[a] Reference 5.

[b] Reference 6.

[c] Reference 7.

Table 3

	ω_i^o	x_{ii}^o	α_i	NS_i
N_2	2359.61 [a]	14.456 [a]	.0187 [a]	1
O_2	1580.36 [a]	12.073 [a]	.01579 [a]	1
$CO_2(Q_1)$ [c]	2349.16 [b]		.00309 [d]	-1
$CO_2(Q_2)$ [c]	1388.17 [b]		.00121 [d]	1
$CO_2(Q_3)$ [c]	667.4 [b]		-.0072 [d]	1

[a] Reference 5.

[b] Reference 8.

[c] The numbering of normal coordinates is that used in the program--$\omega_1 > \omega_2 > \omega_3$--and does not correspond to standard numbering.

[d] Reference 7.

infrared spectra (refs. 5, 7). CO_2 anharmonicities were not used for the spectra given here; however, these data are available and should be used.

β was derived from measurements of the depolarization ratio of the Rayleigh band (including rotational wings) combined with α calculated from refractive index measurements (ref. 6). ATB was derived from the depolarization ratio of the Raman vibration-rotation band, and β' was derived from the latter combined with the intensity ratio of the Raman to Rayleigh bands (ref. 6).

NVM and NJ, the maximum v and J quantum numbers, are given in table 4. They have been chosen to correspond to the level whose population is less than 10^{-6} that of the most populated level, for the given temperature.

Table 4.

T	NVM			NJ		
	298°	600°	1000°	298°	600°	1000°
N_2	2	3	5	40	58	76
O_2	2	4	7	49	69	89
$CO_2(Q_1)$[a]	2	3	4	92	132	170
$CO_2(Q_2)$[a]	2	4	7			
$CO_2(Q_3)$[a]	5	10	18			

[a] The numbering of normal coordinates is that used in the program--$\omega_1 > \omega_2 > \omega_3$--and does not correspond to standard numbering.

APPENDIX

SPECIAL PROBLEM - CO_2

INTRODUCTION

A subroutine and data set has been developed to generate the frequencies and intensities of Raman scattering lines of CO_2 in the 1300 cm^{-1} region. This is to be incorporated into the general program for simulating the Raman spectrum of a combustion system as a function of temperature and number density, described earlier.

The trace scattering contains the predominant features of the vibrational spectrum, since the depolarization ratio, ρ, is .027 (ref. 2) for CO_2, where

$$\rho = \frac{3I_{anis}}{45I_{tr} + 4I_{anis}} \quad .$$

I_{tr} and I_{anis} are the trace and anisotropic scattering intensity, respectively. The trace cross-section for a transition from initial state, Ji, to final state, Jm, is given by

$$\left(\frac{d\sigma}{d\Omega}\right)_{trace}^{Ji,Jm} = (2\pi\omega_R)^4 \gamma_{J_i} |\langle u_m|\alpha|u_i\rangle|^2 \qquad \text{(A-1)}$$

where u_i and u_m are the vibrational wave functions of the initial and final states, and the other quantities are as defined earlier.

The vibrational energy levels, and hence frequencies, of CO_2 are not reproduced by the harmonic oscillator formulae given previously, due to Fermi resonance between ν_1 and $2\nu_2$. It is first necessary therefore to determine the eigenvalues and eigenfunctions of the perturbed Hamiltonian matrix. The unperturbed energy levels and the perturbation terms are calculated using parameters from detailed analysis of infrared spectra (refs. 7, and 13 to 18). The resulting matrix is then diagonalized. In order to insure correct interpretation of the parameters, the energy eigenvalues, first obtained only for the nonrotating molecule, were compared to the calculated and the observed infrared values for 30 levels ranging from 667 to 7603 cm^{-1}.

Two programs were used to perform the calculation: UNPERT, which generates the unperturbed frequencies and quantum numbers, and PERT, which reads the data from UNPERT, sets up and diagonalizes the energy matrix and outputs the energy eigenvalues. PERT was then converted to a LINES subroutine analogous to the rotational and diatomic vibrational LINES subroutines described before. This involved setting up the necessary data in terms of common blocks and arguments consistent with the basic program, solving the energy matrix for eigenvectors as well as eigenvalues, using the former to generate the cross-sections and the differences between the latter to generate the frequencies of the vibrational transitions. At the end of the subroutine the frequency and cross-section arrays are reordered according to increasing frequency in order to be consistent with the C parameter in the CNVLUT subroutine.

Pure vibrational spectra were produced which did not include the dependence of the Fermi coupling terms on the rotational quantum number, J, nor a set of rotational lines for each vibrational transition, which forms the envelope of the vibrational band. A rough simulation of the band envelope was provided by giving a broad (3 cm^{-1}) Lorentzian lineshape to each vibrational transition.

The programs have subsequently been modified to include the rotational structure as follows: the unperturbed values of the

rotational constants, B_v, were generated as a function of the vibrational quantum numbers, according to equation (9), along with the E_v° in program UNPERT. A loop and branch condition were added to the LINES subroutine to provide for explicit calculation of the rotational lines. This involved addition of the J dependence to the Fermi coupling terms and calculation of the perturbed B_v values by averaging over the eigenvectors. These B_v values are used to obtain the rotational contribution to the energy, which determines the rotational Boltzmann factor, and to obtain the rotational part of the frequency according to equations (7) and (8).

It is desirable to test the program at a rotational and vibrational temperature of 1565°K, since an experimental spectrum at this temperature has been published (ref. 10). However, there are approximately 280 vibrational levels occupied at this temperature, each containing up to 145 rotational levels. Since it is not possible to load a two-dimensional array containing this many elements, the program was modified to provide for convolution over the line shape function after the lines for each set of vibrational levels for a given J value (i.e., rotational state) were generated. In this manner all the data is stored in the array of ordinate points (Y array as described earlier), and the same frequency and intensity arrays are reused for each J value. This is accomplished by calling the CNVLUT subroutine from within the loop over J, which is the outer loop in the LINES subroutine. When J = NJ - 1 (NJ is the maximum value of J), control is transferred to the main program where the final call to subroutine CNVLUT is made. Convolution is then performed over the slit function, and the data is sent to subroutine SPKPLOT to produce a plotted spectrum.

At present the unperturbed energy levels as calculated by an independent program are read in by this LINES subroutine.

THEORY

Energy

The expression for the unperturbed vibrational energies is essentially the same as that used before [see eq. (10) in main text], except that the anharmonicity constants are the negative of those defined previously, and it is expressed more simply in terms of the anharmonic frequencies:

$$G^\circ(v_1, v_2, v_3) = \sum_{k=1}^{3} \omega_k v_k + \sum_{k=1}^{3} \sum_{j=1}^{k} x_{jk} v_j v_k + g_{22} \ell^2 \quad . \tag{A-2}$$

The ω_k are related to the harmonic frequencies ω_k° by

$$\omega_k = \omega_k^\circ + x_{kk} d_{kk} + \frac{1}{2} \sum_{j \neq k} x_{jk} d_j$$

where the d_k are the degeneracies of the k^{th} normal coordinate, i.e., $d_2 = 2$, $d_1 = d_3 = 1$. The term in ℓ^2 in equation (A-2) was omitted in reference 1, and the degeneracy of Q_2 was not taken into account.

The theory for the effect of Fermi resonance on the energies calculated by equation (A-2) is essentially that of perturbation theory. Taylor, Benedict, and Strong (ref. 13) showed that the energy levels obtained from infrared spectra could not be fitted unless the Fermi coupling parameters were allowed to vary in a certain way with v_1, v_2, and v_3. Amat and Goldsmith (ref. 20) showed that the variation determined empirically by Taylor et al. is that given by perturbation theory when third-order terms in the transformed Hamiltonian are included. Amat et al. showed that the only nonvanishing matrix elements for this perturbation Hamiltonian

are the off-diagonal elements, $\langle v_1, v_2, \ell, v_3|H'|v_1 - 1, v_2 + 2, \ell, v_3\rangle$, which are also the only nonvanishing elements for the second-order case. Maes (ref. 21) determined the sum of these second- and third-order elements as a function of the quantum numbers to be

$$\frac{\sqrt{[(v_2 + 2)^2 - \ell^2]v_1}}{2}\left[-\frac{k_{122}}{\sqrt{2}} + \lambda_1 v_1 + \lambda_2(v_2 + 2) + \lambda_3\left(v_3 + \frac{1}{2}\right)\right]. \tag{A-3}$$

Although coupling terms exist only between two unperturbed states at a time, any number of states can interact simultaneously. Symmetry requires that all interacting states have the same ℓ and v_3 values. The angular momentum quantum number, ℓ, must be $\leq v_2$ and takes on alternate integer values, being even or odd in accordance with v_2.

The sets of interacting states, or "polyads," are shown systematically for up to $v_2 = 10$ for $v_3 = 0$ in table 1. It is seen that for each value of v_2 there is one polyad each whose degree n is given by

$$n = 1, 2, 3,... \quad \frac{v_2 - \ell_0}{2} + 1$$

where ℓ_0 is the minimum value of ℓ:

$\ell_0 = 0$ for v_2 even;

$\ell_0 = 1$ for v_2 odd.

Referring to the right side of table A1, it can also be seen that for each degree n there is one polyad of that degree for every ℓ value; $\ell = 0, 1, 2,..., \ell_{max}$, where

Table A1. Organization of polyads in terms of unperturbed states (v_1, v_2, ℓ, v_3).

v_2 \ k	1	2	3	4	5	6	ℓ	n
0	$00^{0}0$						0	1
1	$01^{1}0$						1	1
2	$02^{0}0$	100					0	2
	$02^{2}0$						2	1
3	$03^{1}0$	$11^{1}0$					1	2
	$03^{3}0$						3	1
4	$04^{0}0$	$12^{0}0$	200				0	3
	$04^{2}0$	$12^{2}0$					2	2
	$04^{4}0$						4	1
5	$05^{1}0$	$13^{1}0$	$21^{1}0$				1	3
	$05^{3}0$	$13^{3}0$					3	2
	$05^{5}0$						5	1
6	$06^{0}0$	$14^{0}0$	$22^{0}0$	300			0	4
	$06^{2}0$	$14^{2}0$	$22^{2}0$				2	3
	$06^{4}0$	$14^{4}0$					4	2
	$06^{6}0$						6	1
7	$07^{1}0$	$15^{1}0$	$23^{1}0$	$31^{1}0$			1	4
	$07^{3}0$	$15^{3}0$	$23^{3}0$				3	3
	$07^{5}0$	$15^{5}0$					5	2
	$07^{7}0$						7	1
8	$08^{0}0$	$16^{0}0$	$24^{0}0$	$32^{0}0$	400		0	5
	$08^{2}0$	$16^{2}0$	$24^{2}0$	$32^{2}0$			2	4
	$08^{4}0$	$16^{4}0$	$24^{4}0$				4	3
	$08^{6}0$	$16^{6}0$					6	2
	$08^{8}0$						8	1
9	$09^{1}0$	$17^{1}0$	$25^{1}0$	$33^{1}0$	$41^{1}0$		1	5
	$09^{3}0$	$17^{3}0$	$25^{3}0$	$33^{3}0$			3	4
	$09^{5}0$	$17^{5}0$	$25^{5}0$				5	3
	$09^{7}0$	$17^{7}0$					7	2
	$09^{9}0$						9	1
10	$010^{0}0$	$18^{0}0$	$26^{0}0$	$34^{0}0$	$42^{0}0$	500	0	6
	$010^{2}0$	$18^{2}0$	$26^{2}0$	$34^{2}0$	$42^{2}0$		2	5
	$010^{4}0$	$18^{4}0$	$26^{4}0$	$34^{4}0$			4	4
	$010^{6}0$	$18^{6}0$	$26^{6}0$				6	3
	$010^{8}0$	$18^{8}0$					8	2
	$010^{10}0$						10	1

$$\ell_{max}(n) = v_2^{max} - 2(n - 1) \ .$$

Within a given polyad, if we consider the levels as given in the table from left to right, i.e., starting with $v_1 = 0$ and increasing it consecutively by one and decreasing v_2 correspondingly by two, the energy matrix takes on "tridiagonal" form:

$$\left[\langle u_i^\circ | H | u_j^\circ \rangle\right] = \begin{bmatrix} E_1^\circ & W_2 & 0 & 0 \cdots\cdots & 0 \\ W_2 & E_2^\circ & W_3 & 0 & 0 \\ 0 & W_3 & E_3^\circ & W_4 & 0 \\ 0 & 0 & W_4 & E_4^\circ & \\ \vdots & & & \ddots & W_n \\ 0 & & & W_n & E_n \end{bmatrix} \ . \qquad \text{(A-4)}$$

The v_1 and v_2 values may be set up in this order in terms of ℓ, n, and a running index, k :

$$\begin{aligned} v_1 &= k - 1 \\ v_2 &= 2(n - k) + \ell \end{aligned} \qquad k = 0, 1, 2, \ldots n \qquad \text{(A-5)}$$

This index is shown in table A1. The E_k° in equation (A-4) are thus the unperturbed energies calculated from equation (A-2), and the W_k are the coupling terms calculated from equation (A-3), with the k subscripts determining the v_1 and v_2 quantum numbers. Diagonalization of this matrix which yields the correct energy eigenvalues for the polyad characterized by v_3, ℓ, and n, is carried out by the QL algorithm (ref. 22), using the subroutine TQL2, which is available in the CDC math library.

Frequency and Cross-section

The selection rules for the Raman scattering transitions are determined by the symmetry of the polarizability operator and the fact that we are interested in the 1300 cm^{-1} region which corresponds

to transitions, $\Delta v_1 = 1$ or $\Delta v_2 = 2$, for the unperturbed levels. With the Fermi resonance the v_1 and v_2 quantum numbers are no longer valid, and each state in the polyad becomes a mixture of all the unperturbed states in the polyad. Thus, if one state in a polyad can undergo a transition to a state in a second polyad, all the states in the first polyad can undergo a transition to each of the states in the second. Since Q_1 and Q_2^2 are both totally symmetric, symmetry requires that $\Delta \ell = \Delta v_3 = 0$ for the transitions. It can be seen from table A1 that all the transitions for which $\Delta v_1 = 1$, $\Delta v_2 = 0$, and $\Delta v_2 = 2$, $\Delta v_1 = 0$ for the unperturbed states are contained in the conditions $\Delta n = 1$, $\Delta \ell = 0$. Hence the selection rules for the perturbed states are:

$$\Delta \ell = \Delta v_3 = 0$$

and

$$\Delta n = 1 \ .$$

The transition frequencies are determined simply by subtracting the energy of the initial state from that of the final state. The expression for the transition cross-section is obtained from equation (A-1), using

$$u_i = \sum_{j=1}^{n} u_j^{\circ} \, c_{ji} \qquad \text{(A-6)}$$

where the u_j° are the unperturbed wave functions and c_{ji}, $j = 1 \ldots n$, is the i^{th} eigenvector of the matrix in equation (A-4). The relevant terms in the expansion of the polarizability operator $\hat{\alpha}$ are

$$\hat{\alpha} = \left(\frac{\partial \alpha}{\partial Q_1}\right)_o Q_1 + \left(\frac{\partial^2 \alpha}{\partial Q_2^2}\right)_o Q_2^2$$

where α represents the trace of the polarizability tensor as defined before, equation (19) in main text. Representing the u_j by (v_1^j, v_2^j), since it is understood that the ℓ and v_3 quantum numbers of the initial and final states are equal, we have

$$\langle u_m|\hat{\alpha}|u_i\rangle = \sum_{k=1}^{n}\sum_{j=1}^{n-1} c_{km}\, c_{ji}\, \langle(v_1^k, v_2^k)|\hat{\alpha}|(v_1^j, v_2^j)\rangle$$

$$= \sum_{k=1}^{n}\sum_{j=1}^{n-1} c_{km}\, c_{ji}\, \langle(k-1, 2[n-k]+\ell) \qquad \text{(A-7)}$$

$$\times \left|\left[\left(\frac{\partial\alpha}{\partial Q_1}\right)_o Q_1 + \left(\frac{\partial^2\alpha}{\partial Q_2^2}\right)_o Q_2^2\right]\right| (j-1, 2[n-1-j]+\ell\rangle$$

where we now express the v_1 and v_2 quantum numbers in terms of the running index defined in equation (A-5), bearing in mind that the degree of the polyad to which the initial state belongs is n - 1. The sums in equation (A-7) may be separated into two types of terms according to the integrals over the normal coordinates in the unperturbed wave functions. We have (refs. 24, 25)

$$\left(\frac{\partial\alpha}{\partial Q_1}\right)_o \langle v_1+1|Q|v_1\rangle = \left(\frac{\partial\alpha}{\partial Q_1}\right)_o \sqrt{\frac{h(v_1+1)}{8\pi^2\nu_1}} = \langle\alpha_1\rangle^o \sqrt{v_1+1} \qquad \text{(A-8)}$$

where $\langle\alpha_1\rangle^o$ is the integral evaluated for $v_1 = 0$, and

$$\left(\frac{\partial^2\alpha}{\partial Q_2^2}\right)_o \langle v_2+2|Q_2^2|v_2\rangle = -\left(\frac{\partial^2\alpha}{\partial Q_2^2}\right)_o \frac{h}{16\pi^2\nu_2} \sqrt{(v_2+2)^2-\ell^2} \qquad \text{(A-9)}$$

$$= \frac{\langle\alpha_2\rangle^o}{2} \sqrt{(v_2+2)^2-\ell^2}$$

where $\langle\alpha_2\rangle^o$ is the integral evaluated for $v_2 = \ell = 0$. It can be seen that the first type of term occurs for $j = k - 1$ in equation (A-7) and the second type for $j = k$. Accordingly, equation (A-7) reduces to

$$\langle u_m|\hat{\alpha}|u_i\rangle = \sum_{k=2}^{n} c_{km}\, c_{k-1,i}\, \langle k-1|\frac{\partial\alpha}{\partial Q_1}\Big)_o Q_1|k-2\rangle$$

$$+ \sum_{k=1}^{n-1} c_{km}\, c_{ki}\langle 2(n-k)+\ell|\frac{\partial^2\alpha}{\partial Q_2^2}\Big)_o Q_2^2|2(n-1-k)+\ell\rangle$$

where the u^o's are now represented by only one quantum number--that which is different for the two states--v_1 for the terms in the first sum, v_2 for those in the second. The sums over k are altered due to the fact that the sum over j goes from 1 to $n - 1$; thus, there is no $j = k$ term for $k = n$, and no $j = k - 1$ term for $k = 1$. Replacing the dummy index k by $k + 1$ in the first term, we see that it is given by equation (A-8) with $v_1 = k - 1$. The second term is given by equation (A-9) with $v_2 + 2 = 2(n - k) + \ell$. Thus we have

$$\langle u_m|\hat{\alpha}|u_i\rangle = \langle\alpha_1\rangle^o \sum_{k=1}^{n-1} c_{ki}\left[c_{k+1,m}\sqrt{k}\right.$$

$$\left. + c_{km}\frac{\langle\alpha_2\rangle^o}{\langle\alpha_1\rangle^o}\sqrt{(n-k)(n-k+\ell)}\right]. \qquad \text{(A-10)}$$

This quantity is then squared and multiplied by the appropriate factors according to equation (A-1) in order to give the cross-section for the transition.

Rotational Structure

Maes has shown that the Fermi coupling term has significant J dependence for rotational levels with $J > 30$ (ref. 21). These levels will have large populations at the temperatures considered in combustion systems. He has determined the functional form of this dependence to be

$$\delta J(J + 1) \frac{\sqrt{[(v_2 + 2)^2 - \ell^2]v_1}}{2} \quad . \tag{A-11}$$

This term is accordingly added to the W_k in equation (A-4), as given by equation (A-3), when the rotational structure is considered. The eigenvalues and eigenvectors of equation (A-4) will then be different for each J value.

The rotational energies are given by equation (8) in the main text, except that now the B_v values msut be averaged over the wave function for the perturbed states:

$$B_v^J = \sum_{k=1}^{n} (c_{kv}^J)^2 B_k^\circ \tag{A-12}$$

where the J dependence of the eigenvectors and, hence, of the perturbed B_v values is now reflected.

The rotational selection rules for the trace scattering are given by $\Delta J = 0$; hence, the rotational frequencies are given by

$$\omega_J^J = (B_m^J - B_i^J) J(J + 1) \tag{A-13}$$

where i and m represent the vibrational quantum numbers of the initial and final states as before.

The J dependence of the rotation-vibration cross-sections derives from the J dependence of the rotational energies and

hence, of the rotational Boltzmann factor, and the J dependence of the eigenvectors as reflected in the transition polarizability given by equation (A-10). There is no rotational line strength, S_{JJ}, for the trace scattering.

DATA AND RESULTS

The parameters used in the calculations are those determined by Suzuki (ref. 18) (set v) and are given in table A2. They were obtained by a simultaneous fit of the parameters indicated to 33 vibrational band origins and 31 rotational constant differences, $(B_v - B_o)$, observed from infrared spectra. The ground state rotational constant, B_o = .39021 cm, was that used in reference 1, first obtained by Courtoy (ref. 7) and verified by a more accurate measurement (ref. 17).

The comparison of those energy levels obtained by the programs described above, those observed from infrared spectra, and those calculated by Suzuki is shown in table A3. It can be seen that the agreement is reasonable. Further, it can be seen that the agreement is remarkably good between the calculated energies and those observed energies to which the parameters were not fitted (those for which there are no entries in column 2).

In addition to the parameters listed in table A3, the polarizability ratio, $\langle\alpha_2\rangle^o/\langle\alpha_1\rangle^o$, and the value, $\langle\alpha_1\rangle^o$, in equation (A-10) are needed in order to calculate the spectrum. The value of the polarizability ratio was determined from the measurement of the ratio of the Raman intensity of the two fundamental bands carried out by Howard-Lock and Stoicheff (ref. 25). The ratio was obtained using equation (1) of that reference, but using the energy parameters of Suzuki rather than those of Courtoy as did Howard-Lock et al.

The value of $\langle\alpha_1\rangle^o$ was determined from the absolute cross-section measurement of Penney et al. (ref. 12) using the equation

Table A2. Energy parameters of CO_2, cm^{-1} (Suzuki, ref. 18).

	i = 1	i = 2	i = 3
ω_i	1337.55	667.365	2361.62
x_i	-2.94	1.10	-12.47
α_i	.001232	-.000737	.003058
λ_i	.3583	.4975	.2808
x_{12}	-3.64		
x_{13}	-19.66		
x_{23}	-12.37		
g_{22}	-.88		
k_{122}	74.47		
δ	1.9657×10^{-4}		

Table A3. Calculated and observed energy levels for CO_2, cm^{-1}.

Observed	Calculated (Suzuki, ref. 18)	Calculated (present work)
667.38[a]	667.58	667.59
1285.41[a]	1285.60	1285.66
1335.13[a]	1335.51	1335.61
1338.19[a]	1338.03	1338.08
1932.47[a]	1932.80	1932.91
2003.28	2003.88	2004.08
2076.86[a]	2076.66	2076.76
2349.16[b]	2349.16	2349.15
2584.9[b]		2585.74
2672.8[b]		2672.98
2760.75[c]		2760.74
2797.19[c]		2796.84
3004.08[c]		3004.37
3241.5[b]		3241.71
3339.25[c]		3339.73
3341.80	3342.08	3342.33
3502.0[b]		3500.29
3612.84[a]	3612.89	3612.94
3714.78[a]	3714.66	3714.70
4122.7[c]		4122.85
4247.71[a]	4247.97	4248.06
4390.63[a]	4390.68	4390.77
4853.63	4853.56	4853.67
4888.00[a]	4888.55	4888.69

(cont'd.)

Table A3. Calculated and observed energy levels for CO_2, cm^{-1} (concluded).

Observed	Calculated (Suzuki, ref. 18)	Calculated (present work)
4977.81[d]	4977.92	4977.75
5061.78[a]	5062.07	5062.21
5099.61[d]	5099.64	5099.69
5316.09[d]	5316.18	5316.21
5960.08[d]	5959.42	5959.49
6075.93[d]	6075.52	6075.69
6227.88[d]	6227.76	6227.86
6347.81[d]	6348.25	6348.35
6503.05[d]	6503.12	6503.30
6688.54[d]	6687.57	6687.59
6863.91[d]	6863.77	6863.94
6972.49[d]	6972.70	6972.63
7024.03[d]	7024.50	7024.68
7204.22[d]	7204.01	7204.23
7602.85[d]	7603.12	7603.11

[a] Reference 17.

[b] Reference 14.

[c] Reference 5 as quoted in reference 7.

[d] Reference 7.

$$\sigma_{zz} = \frac{3}{3 - 4\rho} (2\pi\omega_R)^4 \, n_{T=298}^{v=0} \, (\langle\alpha_1\rangle^o)^2 \left[1 + \left(\frac{\langle\alpha_2\rangle^o}{\langle\alpha_1\rangle^o} \right)^2 \right]$$

where ρ is the depolarization rato and $n_{T=298}^{v=0}$ is the relative population of the ground state at room temperature. All values used in the equation were those of Penney et al. except for the polarizability ratio, which was determined as described above. It was assumed that the absolute cross-section measurement was over a frequency region including both the fundamental bands. The values determined were

$$\frac{\langle\alpha_2\rangle^o}{\langle\alpha_1\rangle^o} = -.126663 \quad ,$$

$$\langle\alpha_1\rangle^o = 1.2215 \times 10^{26} \text{ cm}^3 \quad .$$

The spectra with and without rotational structure are shown in figures A1 and A2, respectively. The instrument parameters and number density, which determine only the scale of the spectrum and not its relative shape, are the same as those used in the main text. The remaining input data are given in table A4. It can be seen that explicit calculation of the rotational structure makes a substantial difference in the spectrum.

Figure A3 shows the experimental CO_2 spectrum taken by Lapp at 1565°K (ref. 19). It can be seen that the calculated vibration-rotation spectrum is in good agreement with this spectrum.

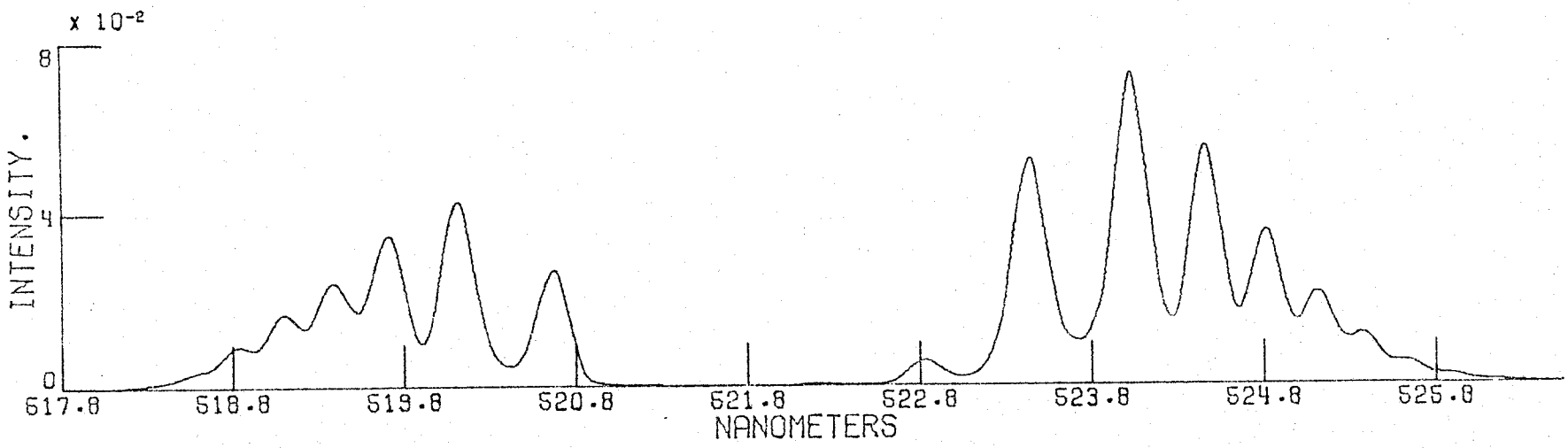

Figure A1. Vibration-rotation spectrum of CO_2 at 1500°K.

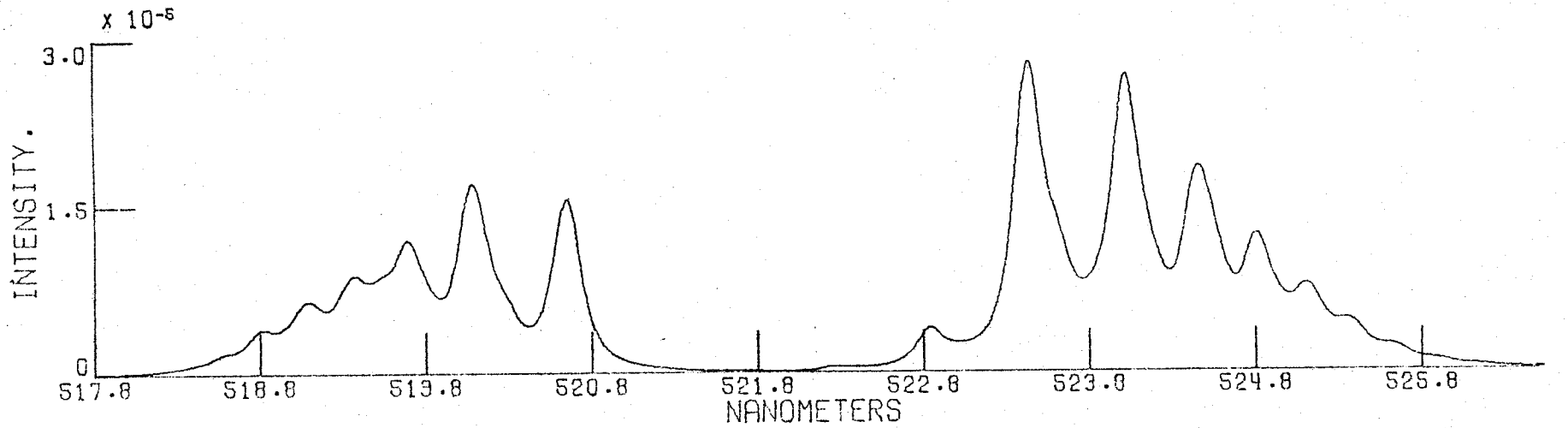

Figure A2. Vibrational spectrum of CO_2 without rotational structure, at 1565°K.

Table A4. Spectral input data for figures 1 and 2.

	$\Delta\nu_{1/2}$	Slit	Temp	v_1 (max)	v_2 (max)	v_3 (max)	J (max)
Fig. 1	0.5 cm^{-1}	3 cm^{-1}	1500°K	4	10	2	144
Fig. 2	3.0 cm^{-1}	1 cm^{-1}	1565°K	4	10	2	

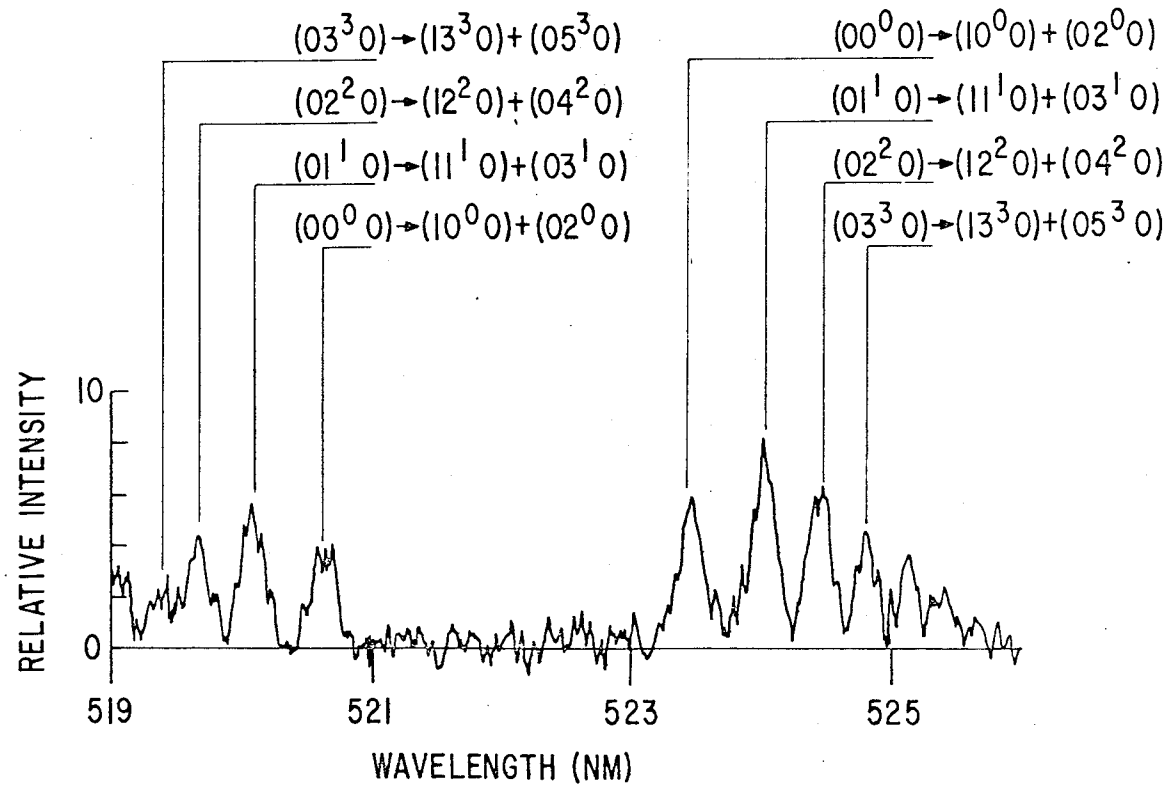

Figure A3. Experimental CO_2 Stokes vibrational Raman spectrum for CO_2 seeded into a stoichiometric H-air flame at about 1565°K, and at a partial pressure of about 1/3 atm. The data were obtained through use of a 1.1w, 488 nm argon ion laser source and a 3/4-meter double monochromator with a triangular spectral slit function full width-half maximum value of 0.163 nm. The notation for the indicated transitions, (v_1, v_2, ℓ, v_3), corresponds to the three fundamental vibrational quantum numbers and to the vibrational angular momentum ℓ of the ν_2-bending mode.

REFERENCES

1. Barrett, J.J. and N.I. Adams: J. Opt. Soc. Am., 58, 311 (1968).
2. Melfi, S.M.: Ph.D. Dissertation, College of William and Mary (1970).
3. Placzek, G. and E. Teller: Z. Physik, 81, 209 (1933).
4. Bribes, J.L., R. Gaufres, M. Monan, M. Lapp, and C.M. Penney: Appl. Phys. Lett., to be published.
5. Herzberg, G.: Spectra of Diatomic Molecules. Van Nostrand Reinhold Co., New York, 1950.
6. Stansbury, G.J., M.F. Crawford, and H.L. Welsh: Can. J. Phys., 31, 954 (1953).
7. Courtoy, C.P.: Can. J. Phys., 35, 608 (1957).
8. Herzberg, G.: Electronic Spectra of Polyatomic Molecules. Van Nostrand Reinhold Co., New York, 1950.
9. Van Vleck, J.H. and V.S. Weisskopf: Revs. Mod. Phys., 17, 227 (1945).
10. Present, R.D.: Kinetic Theory of Gases. McGraw-Hill Book Co., Inc., New York, 1958.
11. Allen, H.C. and P.C. Cross: Molecular Vib-Rotors. Wiley and Sons, Inc., New York, 1963.
12. Penney, C.M., L.M. Goldman, and M. Lapp: Nat. Phys. Sci., 235, 110 (1972).
13. Taylor, J., W.S. Benedict, and J. Strong: J. Chem. Phys., 20, 1884 (1952).
14. Plyler, E.K., L.R. Blaine, and E.D. Tidwell: J. Res. Nat. Bur. Stand., U.S., 55, 183 (1955).
15. Benedict, W.S.: Unpublished work, quoted in reference 7.
16. Amat, G. and H. Pimbert: J. Mol. Spec., 16, 278 (1965).
17. Gordon, H.R. and T.K. McCubbin: J. Mol. Spec., 19, 137 (1966).
18. Suzuki, I.: J. Mol. Spec., 25, 479 (1968).

19. Lapp, M. and D.L. Hartley: In: Combustion Measurements in Jet Propulsion Systems, 133 (1975).

20. Amat, G. and M. Goldsmith: J. Chem. Phys., 23, 1171 (1955).

21. Maes, S.: J. Mol. Spec., 9, 204 (1962).

22. Bowdler, H., R.S. Martin, C. Reinsch, and J.H. Wilkinson: Numer. Math., Bd. 11, 293 (1968).

23. Pauling, L. and E.B. Wilson: Introduction to Quantum Mechanics. McGraw-Hill Co., Inc., New York, 1935.

24. Dennison, D.M.: Rev. Mod. Phys., 3, 280 (1931).

25. Howard-Lock, H.E. and B.P. Stoicheff: J. Mol. Spec., 37, 321 (1971).